FERMILAB-CONF-79-120-E
UPR-70E
Univ. of Pennsylvania
May 1979

HIGH P_T JET STUDIES AT FERMILAB

W. Selove
University of Pennsylvania
Philadelphia, Pa.

ABSTRACT

Two experiments using calorimeters to select and to analyze high p_T events are reviewed. Jets have been seen clearly, and 2-jet events have been found to have all the characteristics expected for parton-parton scattering. Results have been obtained for the structure function of the pion, and for parton transverse momentum. The results are compared with results obtained from di-muon production.

Talk given at the 14th Rencontre de Moriond
Les Arcs, Savoie, France, March 1979

1. INTRODUCTION

High p_T multi-particle events have been studied at Fermilab in three experiments. All three used calorimeters to trigger on high p_T events. I review here results from two of these; data from the third are currently being analyzed. The two experiments are

(1) E-260 Caltech-UCLA-FNAL-UICC-Indiana, and

(2) E-395 Fermilab-Lehigh-Pennsylvania-Wisconsin.

I shall cover E-395 in more detail, since many results from E-260 have been published already for some time. An earlier review of initial results from these two experiments was given by G. C. Fox[1].

Perhaps the major motivation for studying multi-particle high p_T events has been the possibility that one might be able to study parton-parton scattering in this way. No other method of studying parton-parton scattering is known. Following Bjorken et al.[2,3], experiments have studied, first, the question whether "jets" can be clearly seen. In the last 2 years evidence has been obtained clearly showing jet-like properties in high p_T events in hadronic collisions. The next questions addressed have been:

(1) Can jets be defined clearly enough so that the jet momentum vector can be expected to closely correspond to the momentum of a scattered parton?

(2) Can jet pairs be seen clearly, with the properties of p_T-balance and coplanarity expected from a parton scattering mechanism?

(3) If one compares jet pair distributions from πp and pp collisions, does one see the differences expected if these jet pairs indeed correspond to parton-parton collisions?

In the past year or so positive answers have been found to these questions, and the analysis of the data has been carried forward to investigate parton-parton scattering, using 2-jet events.

2. EXPERIMENT E-260

The first experiment to report observation of jet-like events using a calorimeter-triggered detection system was E-260, Bromberg et al.[4,5]. The apparatus used by this group is shown in Figs. 1 and 2. Two calorimeter arms, each of four strips, covering a solid angle of about 1 sr CM in each arm, were used both to trigger on high p_T events and, together with a magnet-and-wire-chamber system, to analyze the events. Two sample events from E-260 are shown in Figure 3. Data were taken at 130 GeV and 200 GeV; detailed results have

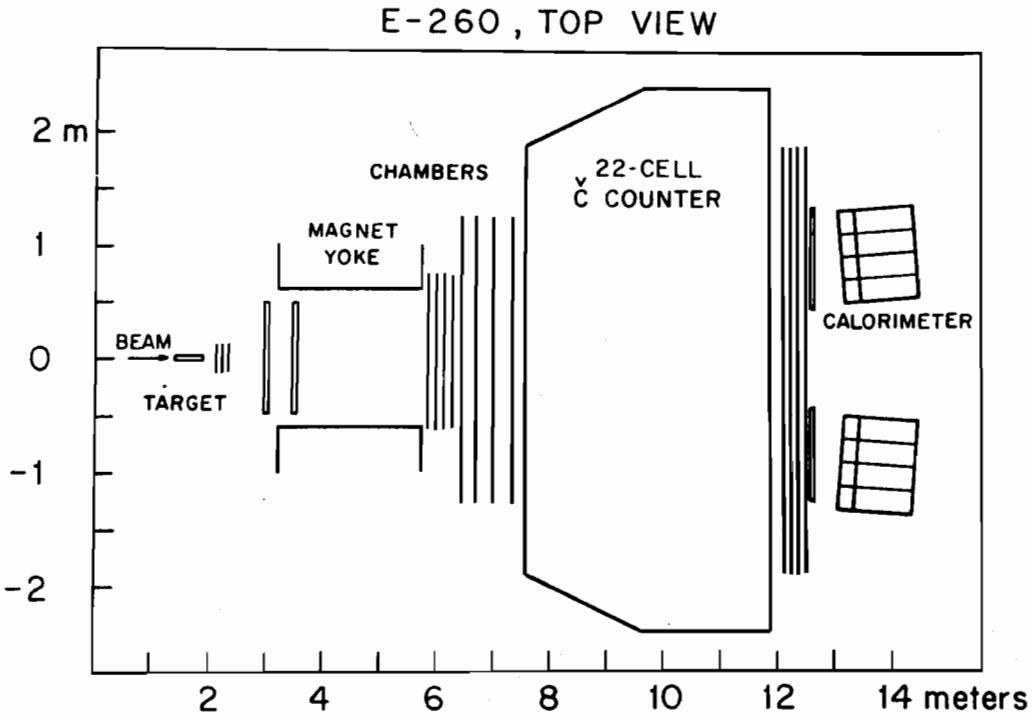
E-260, TOP VIEW
2 m
1
0
-1
-2
BEAM
TARGET
MAGNET YOKE
CHAMBERS
22-CELL Č COUNTER
CALORIMETER
2
4
6
8
10
12
14 meters

FIG. 1

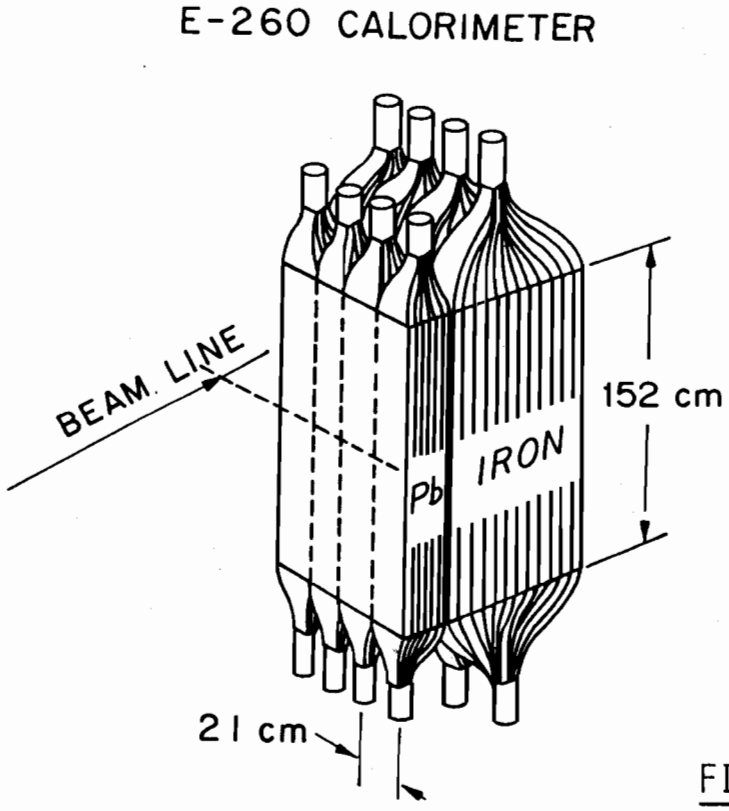
E-260 CALORIMETER
BEAM LINE
Pb
IRON
152 cm
21 cm

FIG. 2

thus far been reported principally for 200 GeV.

Bromberg et al. found a number of important results. Three are emphasized here:

(1) The cross section for multiple-particle groups, "jets", to trigger their calorimeter is more than 100 times larger than the cross section for single particles of the same p_T.

(2) Their typical "jet" event, of total p_T (into the calorimeter) 3 to 5 GeV/c, has about 3 charged tracks entering the calorimeter, along with additional p_T deposition, in general, by neutral particles.

(3) These 3 charged fragments carry, for a 4 GeV/c jet, an average p_T of $\sim$ 0.7 GeV/c each.

In references (4) and (5) Bromberg et al. defined a jet as that group of particles entering the calorimeter (either arm). They give a detailed discussion of the ambiguities in this definition, caused by limited acceptance, by effects of rather modest calorimeter resolution in energy and in space, by magnetic deflection effects which bend some particles into the calorimeter and some out of it, and by uncertainties in effects from "background" particles. They conclude that all of these uncertainties together probably do not change the jet cross section by more than a factor of perhaps 2 or 3, and thus do not affect their basic conclusion that the cross section to produce multi-particle high p_T groups is more than 100 times the sum of all single-charged-particle cross sections. Figure 4 shows, e.g., what they obtain for the invariant cross section, σ(jet), if they use the "raw" energy resolution of the calorimeter, for hadrons, and do not use the much better energy resolution for charged particles which their magnet system provides. One sees that in that case σ would be increased only about 4-fold.

A further property of their jet events discussed by Bromberg et al. is the internal momentum distribution, longitudinal and transverse, among the fragments of a jet. Initial results indicated a very close correspondence between the "fragmentation function" (distribution in longitudinal fractional momentum $p_{\parallel}/p_{jet} = z$) for hadronically-produced jets from beryllium and for lepton produced jets from protons. Recent further results by this group[6] show that there is a pronounced difference in fragmentation functions for jets from hydrogen and jets from a heavier nucleus, aluminum. The exact form of the fragmentation function is of considerable potential importance. First, by comparing lepton-produced and hadron-produced jets one may hope to obtain information on and eventually to test models for the way in which quarks fragment in these physically different environments. Second, in hadronically produced events one expects gluon jets to be produced as well as quark jets; the fragmentation

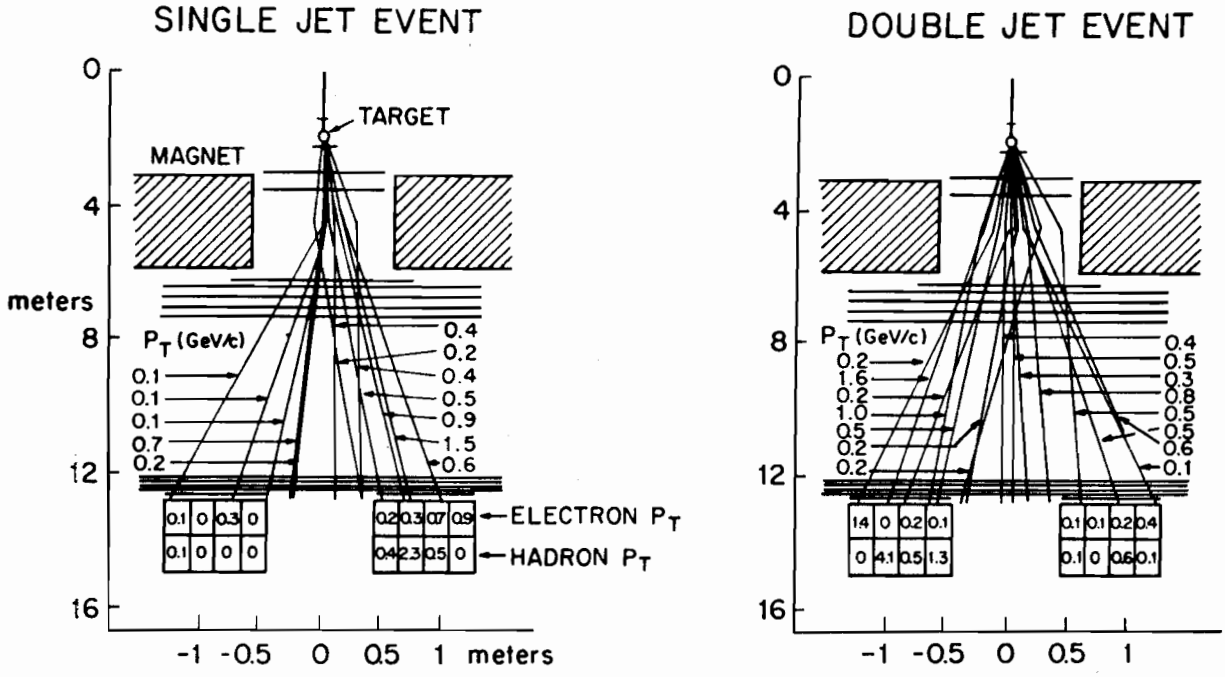

FIG. 3

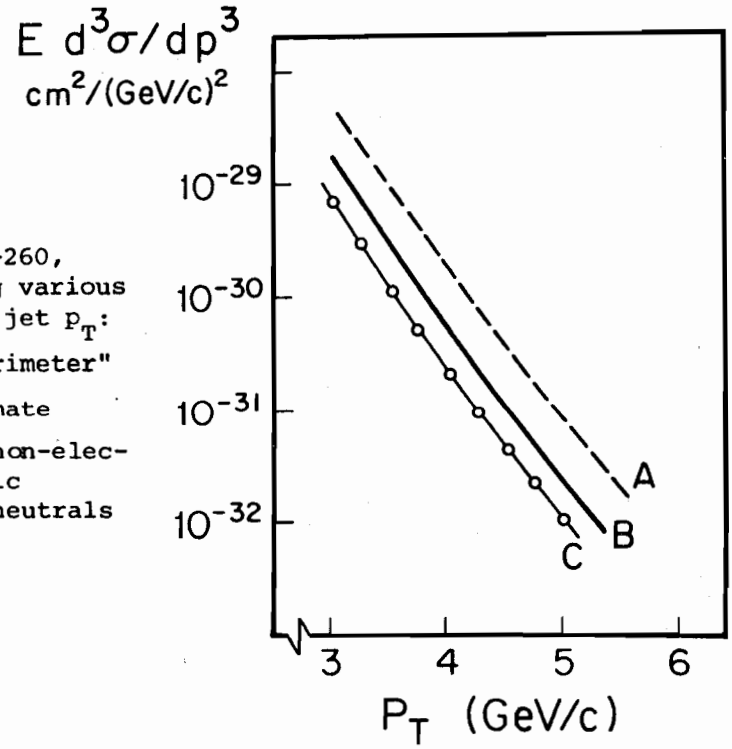

FIG. 4

σ(jet), from E-260, estimated using various definitions of jet p_T:

(A) "raw calorimeter"

(B) best estimate

(C) omit all non-electromagnetic hadronic neutrals

functions for these two types of jets may be distinctly different, and may in fact provide an important tool for distinguishing the two.

* * * *

In the following sections, which discuss primarily results from the other jet experiment at Fermilab reviewed here, E-395, additional features of the E-260 results will be given, comparing results from these two experiments.

3. E-395: APPARATUS

The FLPW collaboration[7] has carried out a high p_T experiment, E-395, with the apparatus shown in Figures 5-7. Initial results are described in references (1), (8), and (9); results from more detailed analysis are given in references (10) to (13).

This apparatus consisted of a 2-arm calorimeter array, segmented in three dimensions, and a set of drift chamber planes. No magnet was used. The two arms could be positioned separately, to cover various solid angle regions at different beam energies. Data were taken at three beam energies--130, 200, and 400 GeV.

The calorimeter array used in E-395 had more comprehensive segmenting than that in E-260. The "right" arm consisted of 25 separate segments (Figs. 6 and 7), each subdivided in depth into four basic layers of modules[8,10,14]. The left arm had 24 segments of electromagnetic calorimeter, followed by more coarsely segmented hadron calorimeter over a large portion of the area. The modules which make up the majority of the calorimeter array use a fluorescent wave shifter light collection technique developed for this type of experiment[15,16].

This calorimeter array has somewhat better energy and p_T resolution than that used in E-260. Thus although E-395 did not have the momentum precision for charged tracks provided by the magnetic analysis in E-260, and although there is a basic resolution problem introduced by the fact that electromagnetic and non-electromagnetic showers give different pulse height spectra for the same energy, it has proved possible to make p_T measurements of multi-particle groups with an effective resolution of about $\pm 8\%$[17].

Finally, the calorimeter array of E-395 covered an appreciably larger solid angle than did that of E-260--about 2 sr in the right arm and 1.5 sr in the left arm.

4. JET CROSS SECTIONS

As noted above the E-260 group concluded that even with the various ambiguities involved in defining a jet their measured invariant cross section,

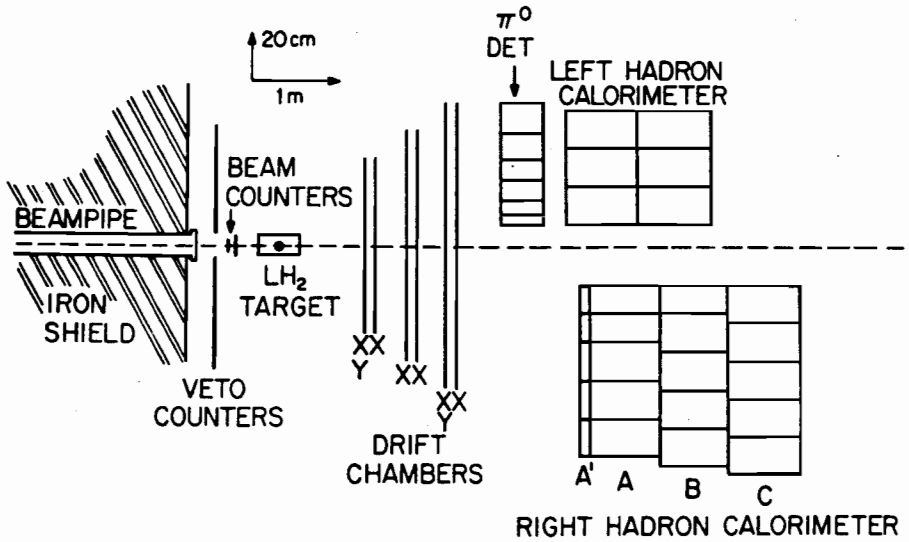

FIG. 5 E-395 , TOP VIEW

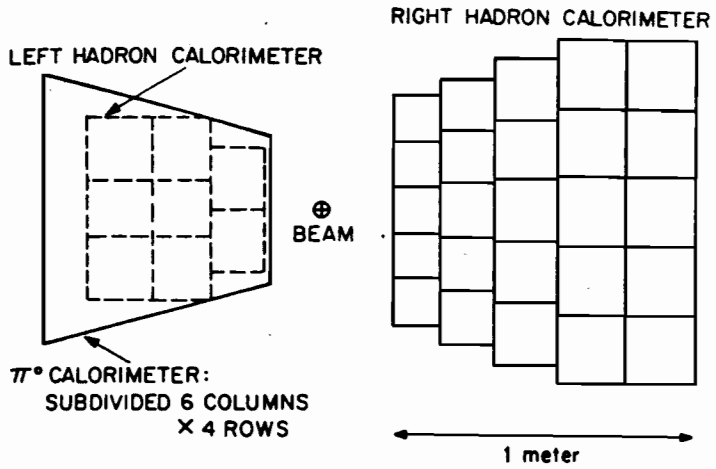

FIG. 6

E-395 , FRONT VIEW

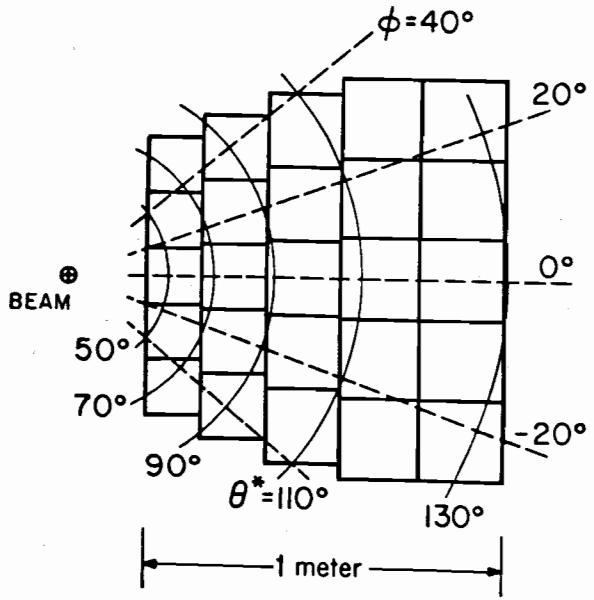

σ(jet), would probably not be changed by more than a factor of 2 or 3 by any reasonable changes in the estimates of the effects of the various uncertainties. The E-395 experiment produced further information on the nature of jets observed with a calorimeter trigger, on the biases involved when such a trigger is used, and on the magnitude of the effects from limited solid angle acceptance (causing jet fragments of wide angle to be missed) and from "background" low-p_T particles (causing the measured p_T to be larger than that due solely to the fragments of the high p_T jet). These matters are discussed in more detail in the next section. Here we compare the magnitude of the jet cross sections reported by the two experiments.

E-260 has reported jet cross sections for 200 GeV hadrons on beryllium[5], and preliminary jet cross sections for 200 GeV protons on hydrogen[18]. FLPW have reported preliminary jet cross sections for pp collisions at several beam energies[13]. We shall compare these cross sections for a sample point, 4 GeV/c p_T at 200 GeV.

First we note that FLPW have studied the effect of detector solid angle, $\Delta\Omega$, on the apparent jet cross section. They find a considerable dependence of σ(jet) on $\Delta\Omega$. To give meaningful cross sections it is therefore necessary to specify the detector solid angle used.

Table I gives the preliminary values of σ(jet) obtained in the two experiments. The agreement is quite respectable, in view of the considerable differences in the two experiments, discussed further below.

One point particularly deserves further comment here. A detector of limited solid angle will give a jet cross section which is only a fraction of the "true" σ(jet). That is, there is a jet detection efficiency factor, which is less than 1, and which decreases with decreasing $\Delta\Omega$. To obtain the "true" jet cross section it is therefore necessary to correct the measured σ(jet) for detection efficiency. This is a rather complex subject, which will be discussed elsewhere. I give here, without details, a rough estimate that this detection-efficiency correction will increase the σ(jet) of Table I (E-395 data) to about 10^{-30} cm^2/(GeV/c)^2.

The cross sections given in Table I can be compared with recent theoretical predictions by Feynman, Field and Fox[20] and by Field[21]. These predictions are based on QCD calculations, substantially modified by parton transverse momentum effects. The theoretical cross sections lie a factor of 2 to 5 above the experimental ones. Considering the uncertainties and differences in the experimental cross sections (a factor of 2 to 4), the detection efficiency factor just mentioned, the fundamental problem that one does not know how to relate the momentum and energy (unequal) of the physical jet to the momentum and energy (equal) of the theoretical scattered parton, the unknown relative properties and

TABLE I. Comparison of Jet Cross Sections at a Sample Point[1]

$pp \rightarrow jet + X$

(p_T = 4 GeV/c; 200 GeV; $\theta^*(jet) = 90^o$)

1. $\sigma(jet)$[1]

Experiment	Calorimeter $\Delta\Omega$	$\sigma(jet)$	Comment
E-260	1 sr	1.3×10^{-31}	Ref. (18)
E-395	2 sr	2.2×10^{-31}	Ref. (13)
E-395	1 sr	0.3×10^{-31}	unpublished

2. $\sigma(jet)/\sigma(\pi)$[1,2]

Experiment	$\Delta\Omega$	$\sigma(jet)/\sigma(\pi)$
E-260	1 sr	300
E-395	2 sr	500

NOTES: (1) $\sigma(jet)$ and $\sigma(\pi)$ defined as $E(d^3\sigma/dp^3)$, in $cm^2/(GeV/c)^2$

(2) $\sigma(\pi) = \frac{\sigma(\pi^+) + \sigma(\pi^-)}{2}$; data from Antreasyan et al.[19]

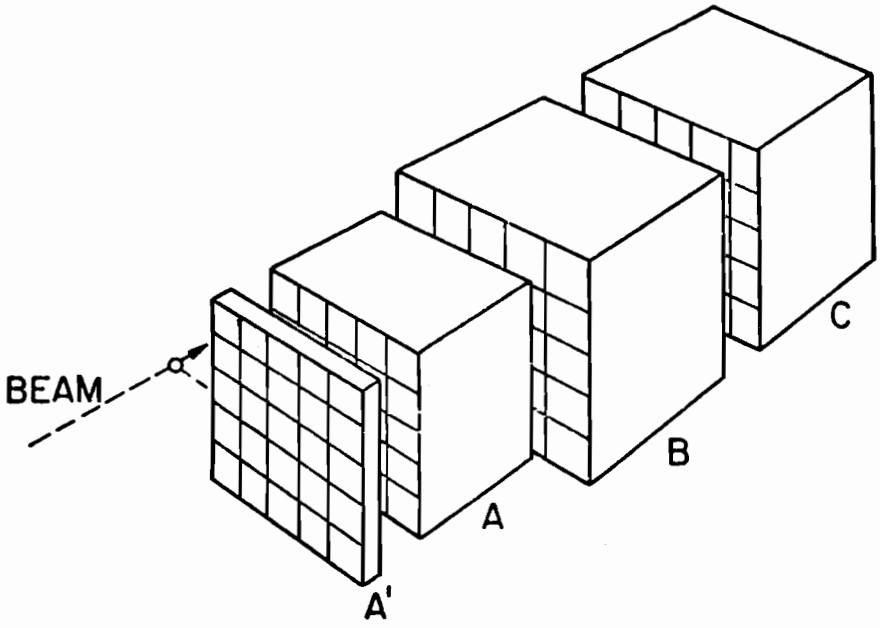

FIG. 7

E-395, SCHEMATIC VIEW OF RIGHT ARM

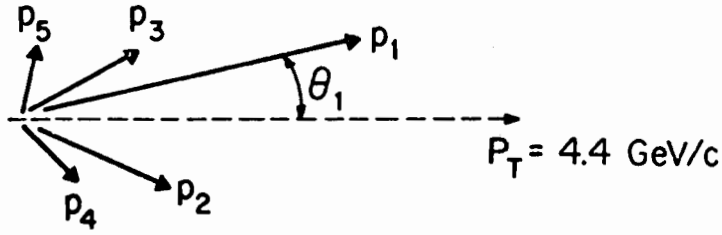

FIG. 8 MODEL JET (SEE TEXT)

fragment	$p_{\parallel}$	θ
1	2.0 GeV/c	10°
2	1.2	16°
3	0.7	26°
4	0.35	46°
5	0.15	66°

detection efficiencies of quark jets and gluon jets, and the uncertainties in the theoretical predictions, the degree of agreement between experiment and these theoretical cross sections is reasonably good.

5. JET STRUCTURE, JET CONTAINMENT, TRIGGER BIAS

A. The large $\sigma(\text{jet})/\sigma(\pi)$ ratio, and questions of jet containment

The calorimeter experiments show that multi-particle high-p_T groups of a given total p_T occur with very much larger cross-section than single particles of the same p_T. Thus correlated groups of particles dominate high-p_T events.

Experimental information on two-particle correlations in high p_T events, at the ISR, already showed some time ago that high-p_T particles occur in correlated groups. This evidence led to the prediction that calorimeter-triggered detection of multi-particle groups should give a cross section much larger than the single-particle cross section[22-28]. Thus, although the exact ratio $\sigma(\text{jet})/\sigma(\pi)$ could not be precisely predicted from the correlation data, large cross sections from multi-particle clusters were to be expected.

How well are these clusters contained, in the existing calorimeter-triggered experiments? How much of the jet momentum is missing? What kinds of trigger bias are present?

B. Rapidity plateau jet model

The existing experiments give considerable experimental evidence on these questions. Before describing some of the experimental information, we sketch the general character that a jet event might be expected to have. The jet event represented corresponds to a model[9] in which the longitudinal momentum distribution $p_{\parallel}$ has a rapidity plateau like that found in SPEAR jets[29], and in which there is a limited internal transverse momentum q_T. The SPEAR jets show evidence of a rapidity plateau with $dN/dy \sim 2$, and show $\langle q_T \rangle$ leveling off at about 1/3 GeV/c at higher E_{jet} values. (Recent accumulating evidence shows similar jet structure in other types of high energy collisions[30-34].

If hadronically produced jets have a structure like that of Figure 8, we see that a detector with a roughly conical acceptance of 2 sr ($\sim 47^{\circ}$ half-angle) would be expected to contain all but the last one or two low-$p_{\parallel}$ fragments, and thus to be missing on the average $\sim$ 0.4 GeV/c in p_{jet} (or $\sim$ 0.8 GeV in E_{jet}). If the acceptance solid angle is instead 1 sr (half-angle $\sim 33^{\circ}$) the missing fragments might carry on the average a total of $\sim$ 1.0 GeV/c in $p_{\parallel}$ instead of 0.4 GeV/c.

C. Experimental information on jet containment in E-395. The Dris effect.

Figure 8 represents a theoretical model of a jet event. In order to study experimentally the character of high p_T events actually observed with a calorimeter trigger, the FLPW group have analyzed a sample of events using the

central part of the right arm, 0.8 sr, as the effective trigger calorimeter. For events which deposit large total p_T in that "inner" part of the calorimeter array, one can then observe the character of that inner deposition; and at the same time one can observe what further particles and further p_T appear in the surrounding "outer" part of the right arm, an additional 1.3 sr.

Figure 9 shows an approximate representation of these inner and outer regions, in CM angles. Figure 10 shows the p_T and multiplicity distributions in the inner and outer regions, for events selected in software as having deposited large p_T in the inner region--approximately 4 GeV/c for Figure 10. In making this selection no conditions were imposed on the p_T present in the outer region[35]. The multiplicity N_{seg} plotted in Figure 10 is defined as the number of segments having p_T greater than 0.3 GeV/c[36].

Figure 10 shows the following result: For events selected by a trigger requirement of 4 GeV/c p_T deposited in 0.8 sr

(a) the 4 GeV/c is carried on the average by about 3 particles--which thus have $\sim$ 1.3 GeV/c each,

(b) there is rather little additional p_T in the surrounding additional 1.3 sr. In the 16 segments of the outer ring there is on the average only about one additional particle. Of the 0.8 GeV/c average p_T in the outer segments about half is estimated to come from spill-over of the showers in the triggering segments, leaving a net outer region p_T of only about 0.4 GeV/c for 1.3 srad.

Thus these calorimeter-triggered events show a very sharply clustered character, with several particles of high individual p_T grouped in a cone of about 30^o half angle, while in the immediate surrounding region of $\sim$ 1½ times as much additional solid angle the additional p_T is only 0.4 GeV/c, about 10% of the triggering p_T.

At first sight it might appear surprising that there is so little p_T in the outer region. However, this result was in effect predicted, by Dris[37]. Dris has pointed out that because of the steeply falling p_T spectrum a calorimeter detector shows a trigger bias, in favor of narrow jets. For a 4 GeV/c trigger in the inner region, calculation with a jet model and with a p_T spectrum falling approximately as e^{-3p_T}[4,8,9] shows that one can expect that on the average the additional jet energy to be expected outside the inner region is only about 1/3 GeV[37,12].

Two important results follow from this Dris effect.

(1) A calorimeter trigger, of 1 sr or more, can measure $\vec{p}_{jet}$ well, even for p_{jet} as low as 2 or 3 GeV/c. (Further experimental evidence supporting this conclusion is discussed below.)

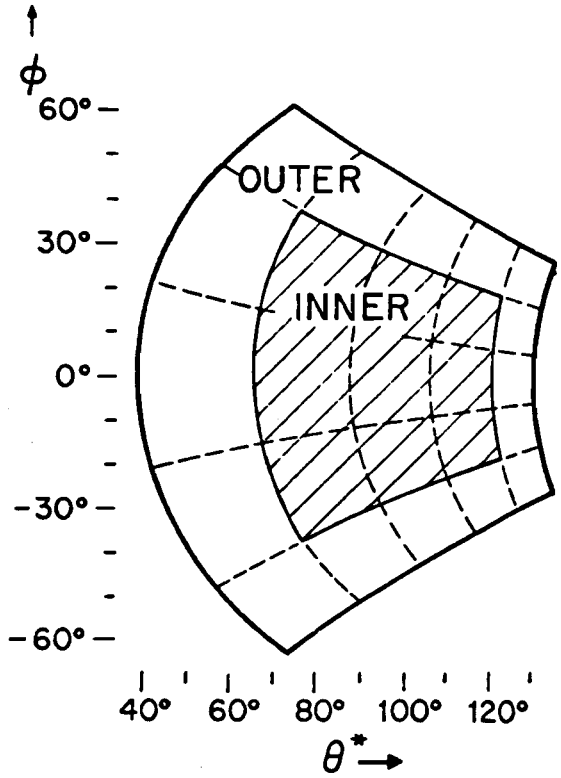

FIG. 9

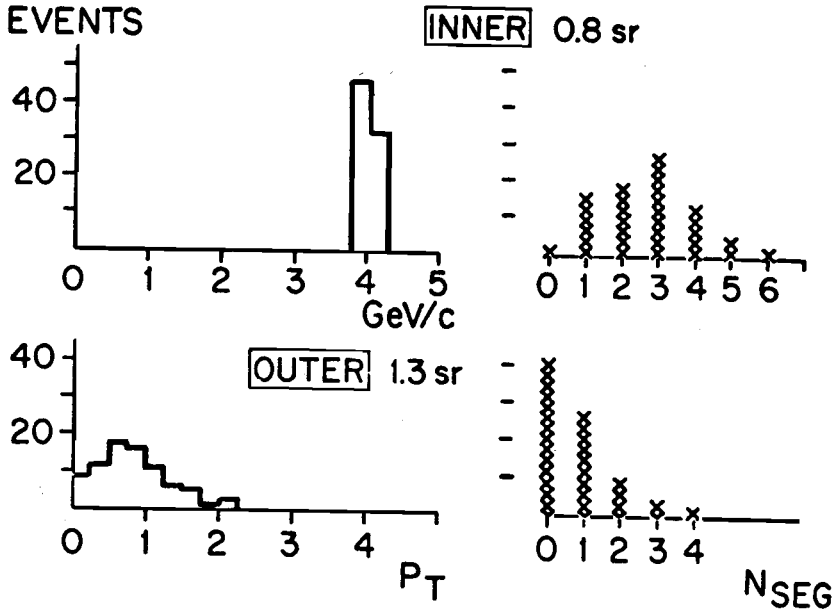

FIG. 10 P_T and multiplicity, in inner and outer regions (Fig. 9), for events triggering with 4 GeV/c in inner region.

(2) The cross section observed, σ(jet), will depend on the detector solid angle, $\Delta\Omega$. A calorimeter triggered detector tends to record only those jets which "fit into" the detector, and the detection efficiency is therefore not 100%.

D. Further remarks on jet properties. Background particles.

Several other conclusions can also be drawn from the results of Figure 10.

(1) Jet structure. For a 0.8 sr detector the 4 GeV/c jets observed correspond to a few particles, each carrying high p_T on the average.

(2) q_T in the jet. The FLPW experiment is not able to obtain very accurate momentum vectors for individual particles, because of the finite granularity of the detector. $\langle q_T \rangle$ can however be estimated roughly, for the events of Figure 10, using the measured multiplicity and using information on the $p_{||}$ distribution obtained in other jet experiments[5,6,29]. The value of $\langle q_T \rangle$ obtained is $\sim$ 0.4 to 0.5 GeV/c.

(3) Background low p_T particles. With the 0.8 sr trigger, near 90^o CM, there is very little background from low p_T particles from the beam jet--the surrounding 1.3 sr shows only an additional 0.4 GeV/c or so, and much of this should probably be interpreted as constituting additional p_T of the triggering jet.

E. Jet containment, and trigger bias, in E-260

Next we comment on some similarities and differences in E-260 and E-395.

Little p_T is observed outside the trigger solid angle, in E-260 as well as in E-395. The E-260 calorimeter arms covered $\sim$ 1 sr each, but the p_T of charged tracks was measured over a much larger solid angle. E-260 give measurements[5] for the charged p_T in a roughly 1 sr region adjacent to the calorimeter's 1 sr. More precisely, they give measurements for the region y = 0 to +1, with approximately a half circle azimuthal coverage. They divide the charged particle p_T in this region into two groups, p_T for those tracks which go into the calorimeter and for those which do not. These measurements show a result quite similar to that obtained by E-395. Namely, those tracks which do not go into the calorimeter carry only $\sim$ 15% as much total p_T as those which do go in.

Thus the E-260 events, like the E-395 events, show that for the typical event there is little p_T outside the calorimeter.

Because of the steep p_T spectrum, events which have an apparent p_T as large as possible compared to the true p_T tend to dominate the data. There is a resulting bias which produces the effect that in general there is little p_T outside the calorimeter. In E-395 the calorimeter responds only to particles produced in the direction of the calorimeter, and this effect tends to select narrow jets (Dris effect). In E-260 there is magnetic deflection which bends some particles into the calorimeter and some out. The result, as pointed out in

reference (5), is that the trigger selectively picks out events in which there is a relatively large number of low-p_T particles which by magnetic deflection can simulate high p_T particles in the trigger.

This magnetic-deflection trigger bias gives two effects worth noting.
(1) For a given trigger p_T threshold setting, a large fraction of triggering events have p_T below the trigger threshold. Figure 11 shows this effect. Figure 12 shows the corresponding plot for E-395[8]; here the events cut off fairly rapidly below hardware threshold.
(2) The charged-particle multiplicity in the E-260 events is larger for events of lower total p_T[5], presumably because the lower-p_T events have been more strongly "promoted" by having low-p_T fragments magnetically deflected into the calorimeter.

Thus the magnetic-deflection trigger bias increases the charged-particle multiplicity in the events which trigger in E-260, and reduces the average p_T per charged particle, over the values which would be observed without such a magnetic effect. Presumably the internal angular spread in the jets is also increased, and the direction of the jet vector is spread (smeared), by this magnetic effect. It is possible that this magnetic trigger-bias effect accounts in part for the difference in σ(jet) values indicated in Table I for E-260 and E-395, but it is difficult to make a quantitative estimate.

F. Summary of jet characteristics. Jet momentum resolution.

The most important result emerging from the preceding discussion is that calorimeter triggered high p_T events at Fermilab energies show evidence of well-defined well-contained jets. This evidence is found to varying degrees both in E-395 and in E-260, and is readily understood through the trigger bias effect pointed out by Dris. When the solid angle of the calorimeter trigger is of the order of 1 sr, it appears that

(a) jet momentum and energy for those jets which are detected are given correctly to a few tenths of a GeV,--i.e., missing fragments of the jet carry no more than this amount of momentum and energy, on the average,
(b) jets of 3 to 5 GeV/c consist on the average of a few particles, each of relatively high p_T ,
(c) "background" contributions to the measured p_T are no more than a few tenths GeV/c per sr, for jets near 90° CM.

The resolution for these jets includes contributions from finite spatial and energy resolution of the calorimeter, as well as from missing fragments, background fragments, and, in case magnetic deflection is used, magnetic smearing effects. Typical values for all of these effects together appear to be of the order of 10% for the p_T of individual events in the 3 to 5 GeV/c range, for experiments E-260 and E-395, and less than that when averaged over many events.

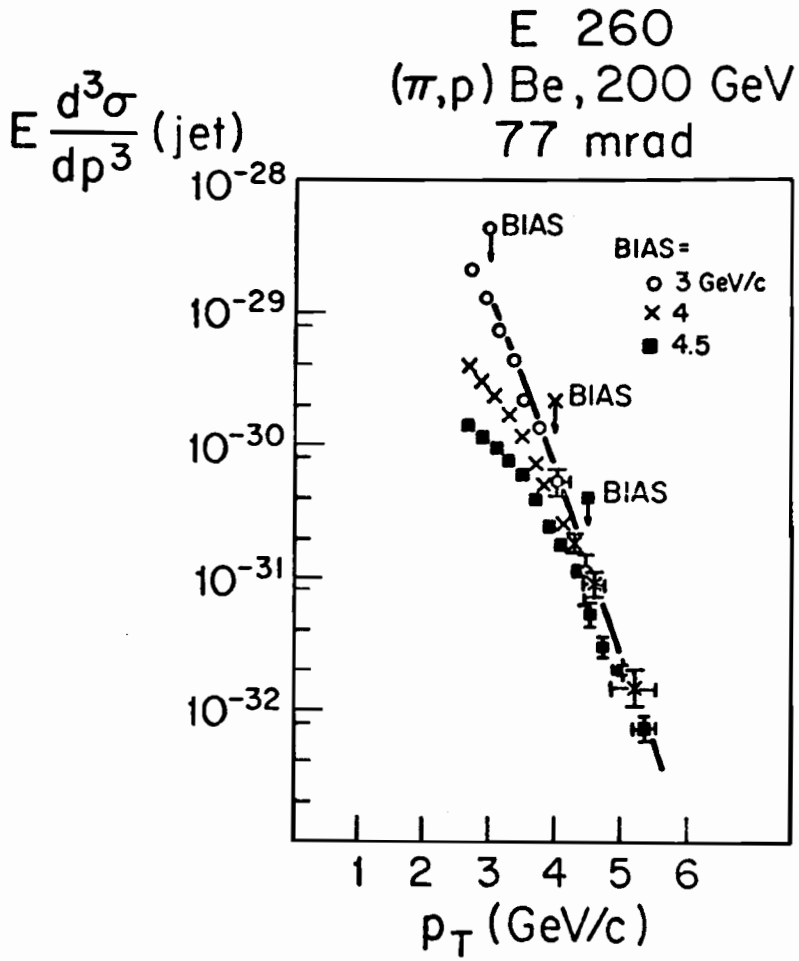
E 260
(π,p) Be, 200 GeV
77 mrad
$E\frac{d^3\sigma}{dp^3}$ (jet)
10^{-28}
10^{-29}
10^{-30}
10^{-31}
10^{-32}
BIAS
BIAS=
o 3 GeV/c
× 4
■ 4.5
BIAS
BIAS
1 2 3 4 5 6
p_T (GeV/c)

FIG. 11

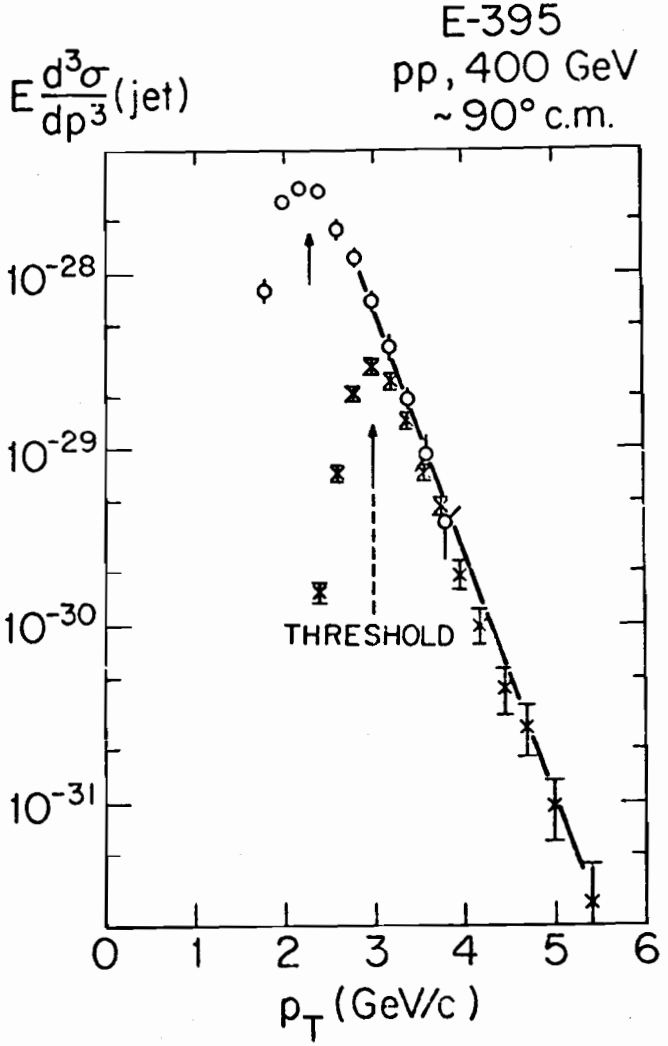
E-395
pp, 400 GeV
~90° c.m.
$E\frac{d^3\sigma}{dp^3}$ (jet)
10^{-28}
10^{-29}
10^{-30}
10^{-31}
THRESHOLD
0 1 2 3 4 5 6
p_T (GeV/c)

FIG. 12

6. THE AWAY-SIDE DISTRIBUTION. P_T BALANCE, COPLANARITY.

If high p_T jets correspond to parton-parton scattering, then the p_T of a jet in one arm should be approximately balanced by a high p_T jet in the other arm. In E-395 an approximate p_T balance of this kind has been observed for the first time.

A. The away-side p_T distribution

Information on such an approximate balance comes first from a study of the away-side p_T distribution, using a single-arm trigger. The left arm (the somewhat smaller one) is used as a trigger, and the away-side distribution in the right arm is then studied. The left jet is selected to have total p_T between 3.95 and 4.2 GeV/c, and to have the jet momentum vector lying in a fiducial region, 60° to 80° in θ^* and $180^\circ \pm 10^\circ$ in ϕ. ϕ is defined as zero in the center of the right arm--see Figure 6. Figure 13 shows two plots of p_T (away) (= p_T (right)) for this selection: A shows p_T (away) for all events satisfying the above cuts on p_T(left), and B shows p_T(away) for those events which in addition have p_T(right) in the central fiducial region of the right arm ($\theta^*_R = 75^\circ$ to 95°, $\phi_R = \pm 10^\circ$).

The away-side p_T spectrum is thus seen to show a peak. For different choices of p_T(trigger), the position of the away-side peak tends to follow, remaining at about 2/3 of the trigger p_T over a wide range of p_T(trigger) values[8,9,12,38]. As discussed in B, below, the away-side p_T is carried, in general, by a multi-particle cluster, with jet-like properties similar to those of the triggering jet. Figure 13 shows that with a 20° x 20° restriction on θ^* and ϕ for the away-side jet, 1/4 of the triggering events still survive. The facts that such a high percentage survive this angle cut, that the away-side p_T spectrum shows a peak, and that the away-side peak p_T value follows the trigger-side p_T value, are all indications of a strongly correlated two-jet structure in these events[8,9,12].

E-395 is the first high p_T experiment to see an approximate balance in (wide angle) high p_T on the two sides of the beam. Most other experiments have not used calorimeters, so have not been sensitive to neutral hadrons; and most other experiments have reported the away-side p_T for only a limited sub-set of the away-side-particles--charged only, for example, or only summed over particles above some minimum p_T. In fact, preliminary data from the recent CCOR experiment show that when away-side π°'s are added to away-side charged p_T the away-side spectrum undergoes a marked change in shape, and begins to show a hint of an away-side peak[39].

Experiment E-260 did use calorimeters, and in principle should show an away-side peak if E-395 shows one, but has not reported seeing such a peak. According to G.C. Fox[40], E-260 did not have a large enough $\Delta\Omega$ in its

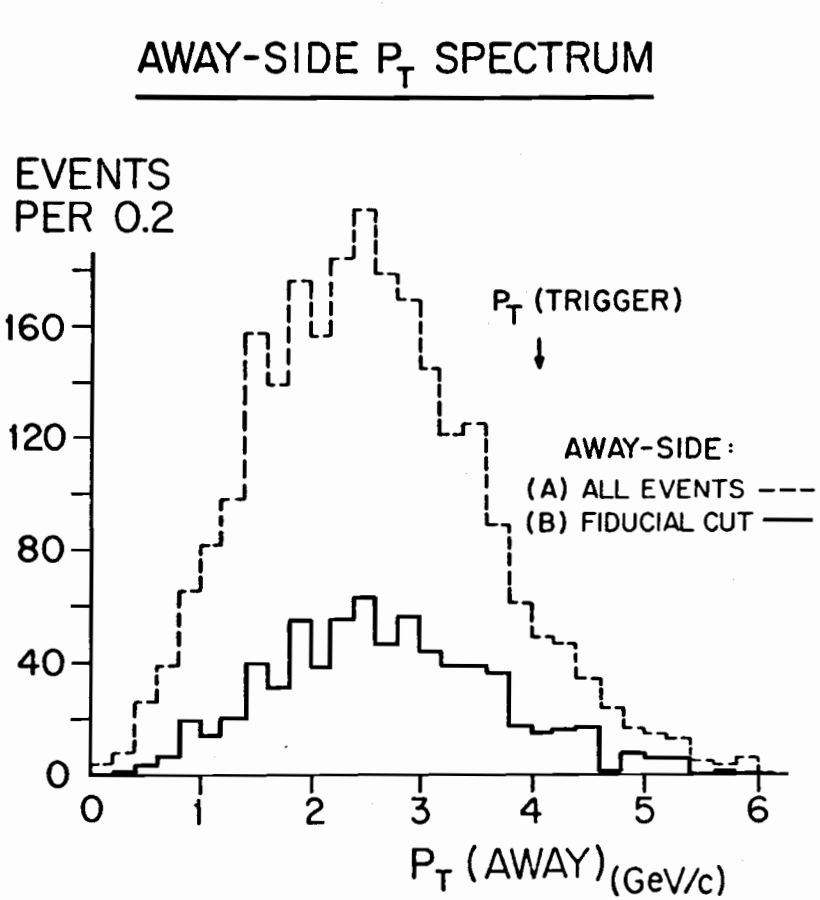

FIG. 13 Away-side p_T spectrum for p_T(trigger) = 4 GeV/c

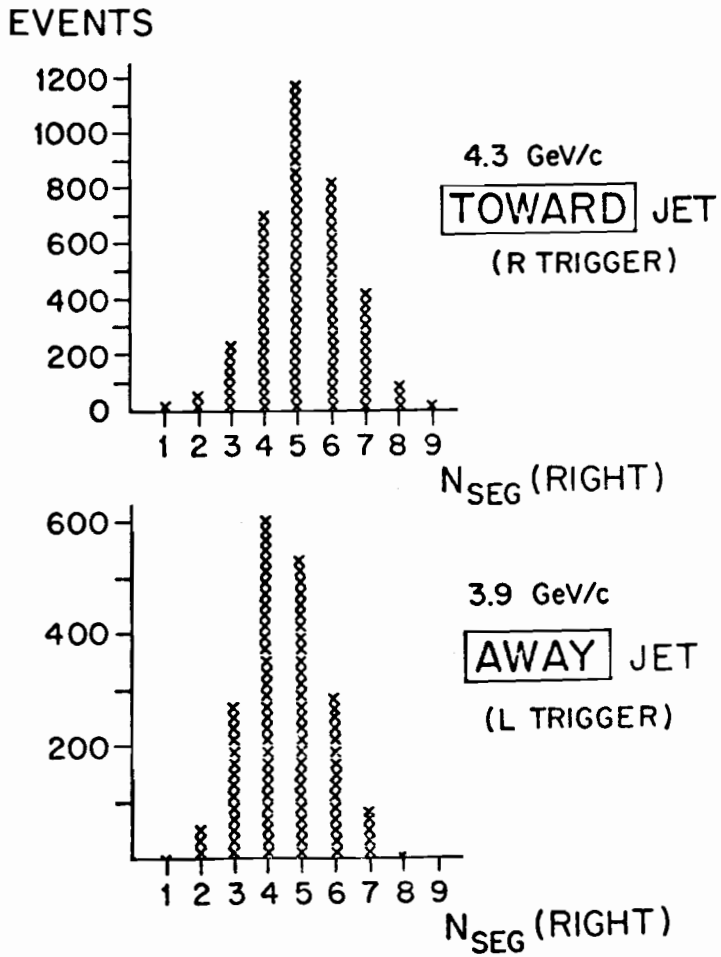

FIG. 14 Multiplicity distributions for trigger-side jet and away-side jet. In (b) the trigger jet and away jet both have $(p_T)_{ave}$ = 3.9.

calorimeter to see such a peak. It may also be that the magnetic-deflection effect in E-260 smears the away-side p_T spectrum and to some extent washes out any peak.

In a parton scattering model the fact that the peak in the away-side spectrum occurs at a p_T lower than the trigger p_T is to be expected, from parton transverse momentum effects, which produce a trigger bias in a single-arm trigger[4,41,42]. Parton transverse momentum information is discussed in detail below.

B. Trigger-side and away-side multiplicity distributions

When a single-particle trigger is used, the trigger side multiplicity is quite low, and changes little with p_T, while the away-side multiplicity is much larger and increases with p_T[43-45]. The low trigger-side multiplicity has a simple interpretation as being due to a trigger-bias effect[41,46]; it could also indicate the presence of a qM (quark plus meson) scattering mechanism, like that of Brodsky, Blankenbecler and Gunion[47].

When a jet trigger is used, how do the multiplicities compare on the trigger side and the away side? Figure 14 shows a result for a sample of data examined by the E-395 group. Multiplicities are shown for the right (R) arm when fiducial-angle and p_T cuts are made on that arm. Figure 14a shows the multiplicity distribution $N_{seg}(R)$ when the trigger is an R trigger (right arm p_T), and Figure 14b shows $N_{seg}(R)$ when the trigger is an L trigger; fiducial-angle and p_T cuts on the right arm are the same for the two plots. No appreciable difference is seen: the away-side jet and the toward-side jet are very similar[48].

C. Double arm "L+R" trigger. P_T balance.

The single-arm trigger gives an away-side peak in p_T, but at a value below the trigger p_T. The difference in p_T values is presumably due to a trigger bias effect, which favors initial parton transverse momenta that contribute to the trigger p_T. In order to remove that trigger bias, E-395 took data with an additional trigger, an "L+R" trigger, which did not favor either arm. This trigger used a two-arm-sum, hardware-produced, to trigger on events in which the sum of the p_T magnitudes in all the modules of both arms together exceed an adjustable threshold.

Figure 15 shows a sample of data taken with the L+R trigger, after application of a further threshold software cut on the sum of magnitudes of the p_T vectors in the two arms, PTL + PTR[49].

Figure 15 shows a marked tendency for the events to cluster near the diagonal--i.e., for PTL and PTR to approximately balance. (For the data shown in Figure 15 the two detector arms were positioned so as to cover quite similar angular regions in the CM). The relatively sharp character of this balance is

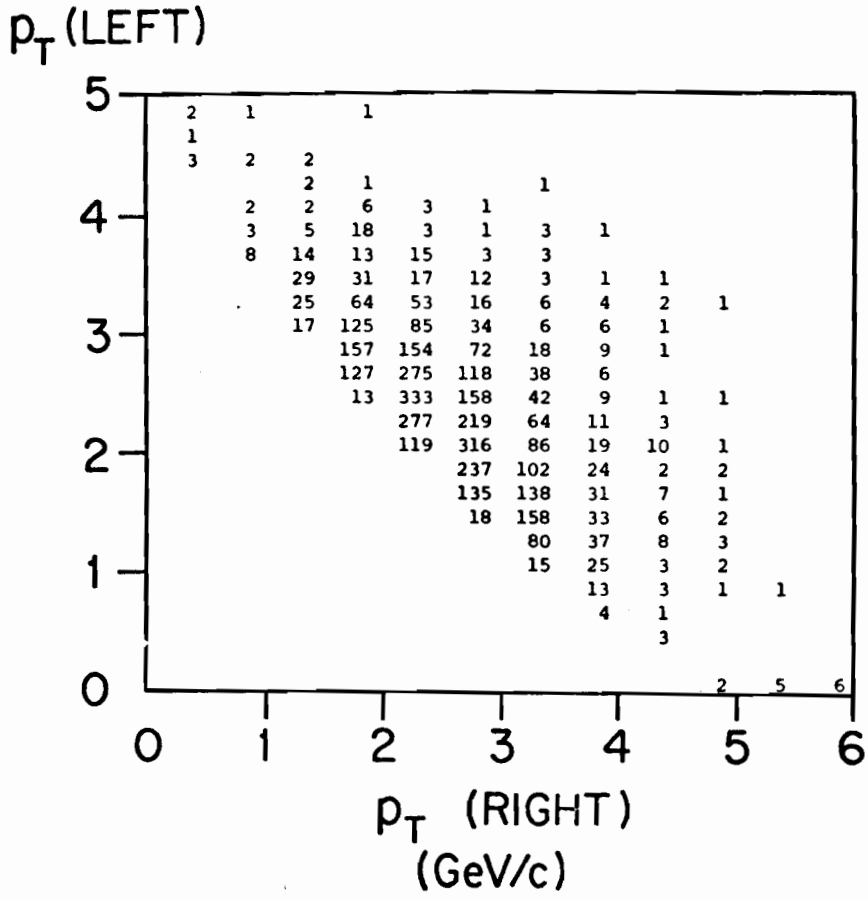

FIG. 15

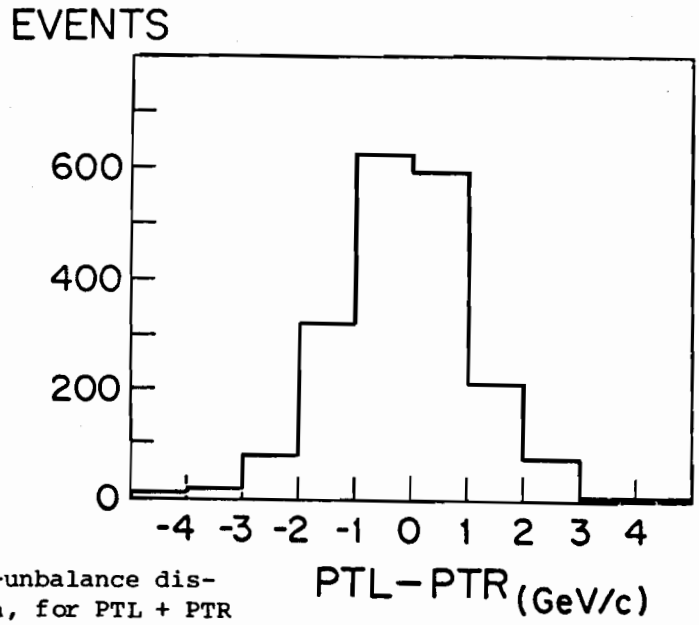

FIG. 16 P_T-unbalance distribution, for PTL + PTR = 4.5 to 5.0 GeV/c.

shown by plotting the density of events in a "cross-diagonal" band, in which PTL + PTR is approximately constant. (Such a band corresponds approximately to fixed parton-parton momentum transfer, in a parton scattering model.) Such a plot is shown in Figure 16, for the band with PTL + PTR between 4.5 and 5.0 GeV/c. This plot shows a FWHM of about 2.4 GeV/c, corresponding to a standard deviation of about 1 GeV/c. In a parton scattering model the standard deviation in this plot is found to correspond to 1.2 to 1.3 times the rms transverse momentum of the partons which undergo a hard scattering. This subject is discussed in further detail below.

It is important to note that the tendency of the events to cluster in the vicinity of p_T balance is not forced by any aspect of the detector, trigger, or analysis. The data have been compared with a model of totally uncorrelated double arm events, in which each arm has an independent p_T spectrum corresponding to the known single-particle high p_T spectrum[9,12]. For such a totally uncorrelated model the density of events is a minimum near the diagonal in contrast to the experimental results, which show a maximum. Thus, although this simple model includes no provision for the possible effects of momentum conservation, the contrast with the experimental results again indicates that a strongly correlated 2-jet structure is being observed.

D. Coplanarity

It has long been known, from ISR experiments, that when one triggers on high p_T there is a marked coplanarity effect for the away-side particles observed[50]. For a jet trigger, the away-side p_T also shows a substantial coplanarity effect, as is qualitatively clear from the fact that plot B in Figure 13 contains 1/4 of the events in plot A. Figure 17 shows more direct evidence of a coplanarity character, for the L+R events. The correlation between ϕ_L for the left-arm jet vector and ϕ_R for the right-arm jet vector is seen to be substantial; but the correlation is not perfect, because of calorimeter acceptance effects. A more detailed discussion of these acceptance effects is given in reference (11).

7. 2-JET ANGULAR CORRELATIONS, AND EVIDENCE FOR PARTON-PARTON SCATTERING.

The p_T balance and coplanarity for jet pairs, discussed in Section 6, are consistent with a parton-parton scattering mechanism, but they do not by themselves prove that to be the mechanism. Specifically, the requirement of momentum conservation might by itself give rise to p_T-balance and coplanarity effects.

If jet pairs are indeed produced by a parton scattering mechanism, then a further important effect must be expected, when jet-pair production is compared

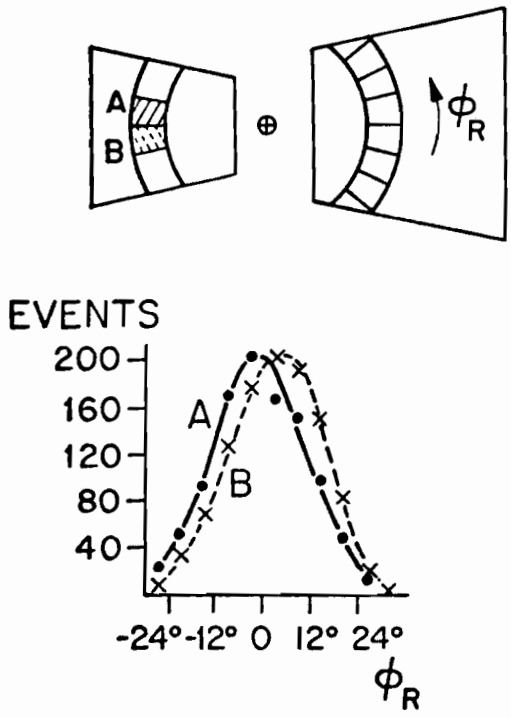

FIG. 17 COPLANARITY RESULTS

FIG. 18

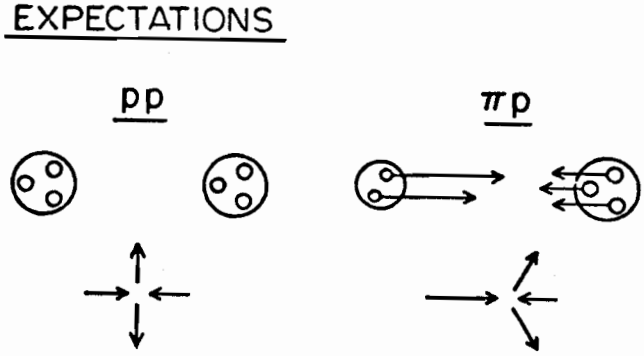

for πp and pp collisions. Namely, the jet pairs from πp collisions should go more "forward", on the average, than the jet pairs from pp collisions. Naively, such an effect is expected, from quark-quark collisions at least, because the pion has only two valence quarks while the proton has three, so that on the average the pion's quarks carry a larger fraction, x, of the incident hadron momentum then do the proton's quarks. This expected effect is illustrated in Figure 18.

The FLPW group examined the 2-jet data from E-395 for such an effect. The results are given in terms of $R_{2\text{-jet}}$, the ratio

$$\frac{\sigma(pp \rightarrow \text{jet} + \text{jet} + X)}{\sigma(\pi p \rightarrow \text{jet} + \text{jet} + X)}.$$

$R_{2\text{-jet}}$ is shown in Figure 19 as a function of θ_L^* and θ_R^*, the CM polar angles of the two jet vectors[10]. At small θ_L^* and θ_R^* there is a larger cross section for pion-induced events ($R < 1$), and at larger θ_L^* and θ_R^* there is instead a larger cross section for proton-induced events ($R > 1$).

Thus pions produce correlated two-jet events at more forward angles than do protons. While p_T balance alone might have been produced simply by momentum conservation effects, the difference in angular correlation for pion-induced and proton-induced jet pairs cannot be produced by such effects. It is the π/p angular correlation difference, taken together with the p_T balance and the coplanarity effects, which gives strong evidence that the jet pairs come from collisions of constituents, and that the constituents of the pion which produce these events have on the average a significantly higher fractional momentum x than those of the proton.

Are these constituents partons--quarks and gluons? Or is there a significant contribution to these events from interactions of more complex constituents, as in the CIM model of Blankenbecler et al.[47]? Although there is not yet a definitive answer to this question, I believe there is an accumulation of evidence that in the jet-triggered events the CIM mechanism does not give a dominant contribution[4,51,52]. If the 2-jet events are indeed due to parton-parton scattering, one still wishes to know the relative contributions of quark scattering and gluon scattering. The possible contribution from gluon collisions is discussed further below.

8. π/p DIFFERENCES IN ONE-ARM JETS. FURTHER EVIDENCE ON JET CONTAINMENT.

If jets come from parton collisions and if the pion has higher momentum constitutents then the proton, then single-arm jets of high p_T, and

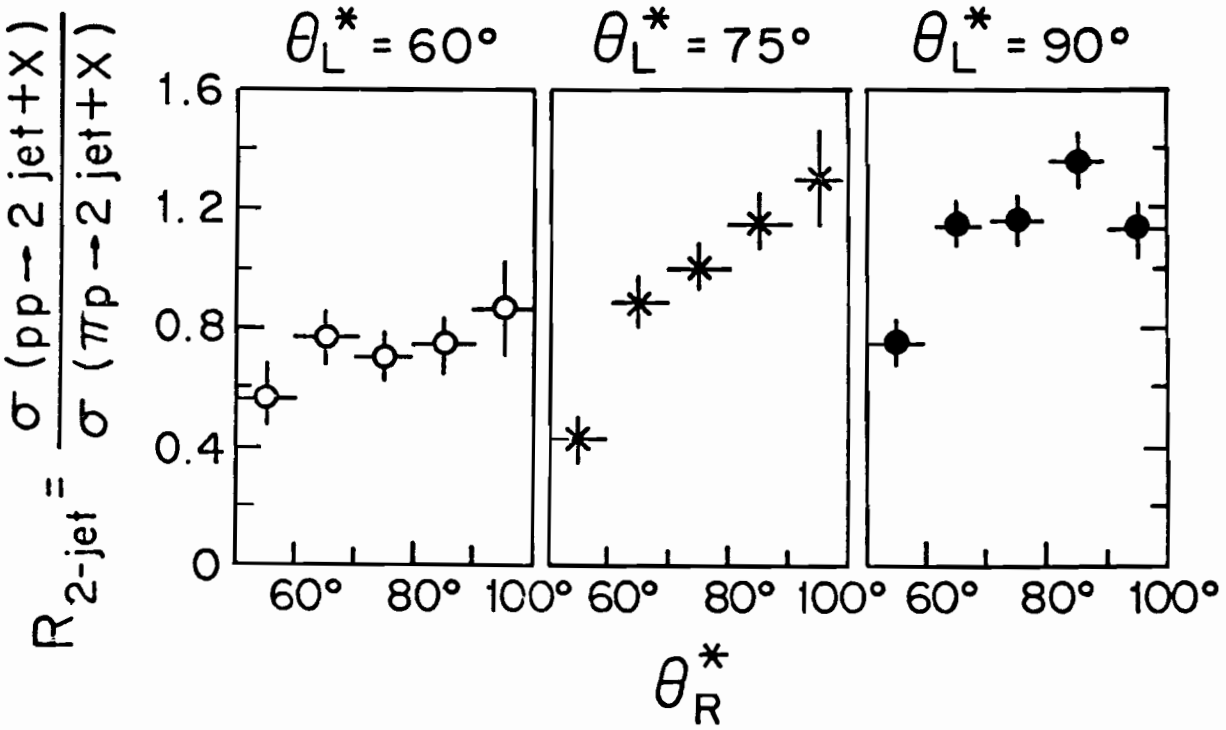

FIG. 19 2-JET ANGULAR CORRELATION RESULTS, PROTON/PION COMPARISON.

individual high-p_T particles also, should be produced more readily by pions then by protons. Evidence of such an effect, for inclusive single π^o's, was first found by Donaldson et al.[53]. Similar clear evidence of such an effect for jets has also been found, by both E-260[1] and E-395[10]. We now discuss that evidence.

Figure 20 shows data points for the ratio R_{jet}, defined by

$$R_{jet} \equiv \frac{\sigma(pp \to jet + X)}{\sigma(\pi p \to jet + X)} \equiv \sigma_p/\sigma_\pi \tag{8.1}$$

for single-arm jets near 90^o CM, as obtained by E-395. Figure 20 also shows (solid curve) the form of the p/π ratio for inclusive π^o's,

$$R_{\pi o} = \frac{\sigma(pp \to \pi^o + X)}{\sigma(\pi p \to \pi^o + X)} \tag{8.2}$$

from Donaldson et al.[53,10]. Results of generally similar character for R_{jet} have also been obtained by E-260[1,18].

In figure 20, the ratio R_{jet} (8.1) is seen to follow a curve which has a shape similar to that for $R_{\pi o}$ but shifted to higher x_T. The dashed curve has been drawn by shifting the solid curve to the right by a factor of 1.4 in x_T. The fact that this simple shift gives a new curve which fits the jet data quite well suggests that a rough scaling exists between the x_T for a given value of R and the single π^o x_T for the same R[54].

The behavior of R_{jet} in figure 20 involves the folding of several effects. First, for each value of x_T the value of R_{jet} does not correspond to a unique value of incident parton fractional momentum x_1 nor of target parton x_2, but instead involves an integral over the parton x-distributions, with appropriately varying parton distributions (structure functions) and parton-parton scattering cross sections. Second, partons of different species are presumably contributing to the jet cross sections which enter into (8.1). R_{jet} therefore involves a sum and integral over the different species of parton-parton collisions. In this sum not only the structure functions and parton-parton cross sections enter, for each species of collisions, but also the possibly different detection efficiencies for jets of different species.

In order to study the possible effect of differing detection efficiencies--i.e., different jet containment factors--for different species of jets, and in fact to study whether πp and pp collisions might produce noticeably different types and "sizes" of jets, the E-395 group have studied the ratio R_{jet}, and individual jet containment effects, for proton-induced jets ("proton jets") and pion-induced jets ("pion jets")[11]. A sample of the results is shown in Fig. 21. Figure 21 shows the event rate, $dN/d\phi_R$, for jets of a given p_T ($\sim$ 2.5 GeV/c) and given θ^* ($\sim 85^o$), as a function of the distance of the jet

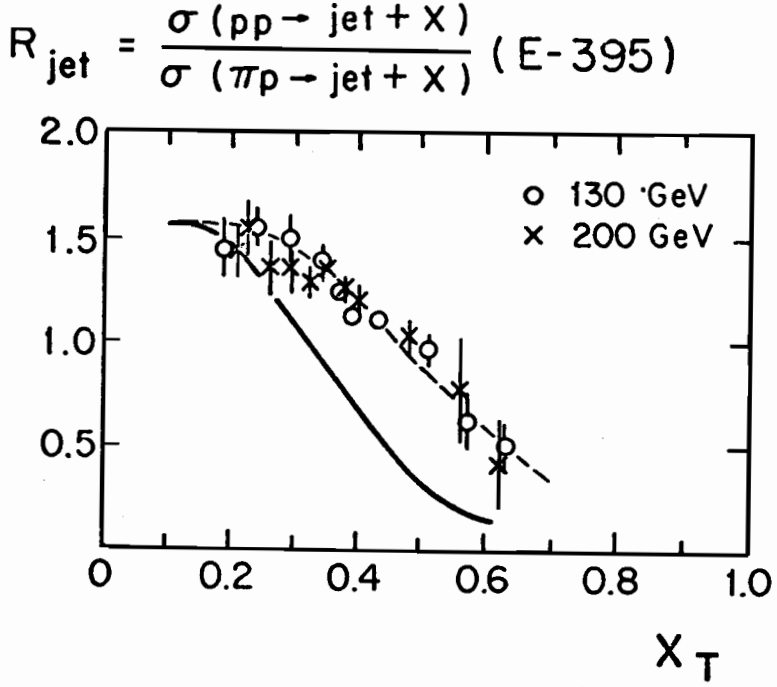

FIG. 20 Data points give R_{jet}, the p/π cross section ratio for jets, near 90°. The solid curve gives $R_{\pi o}$ (see text). The dashed curve is the solid curve shifted to the right by a factor of 1.4 in x_T.

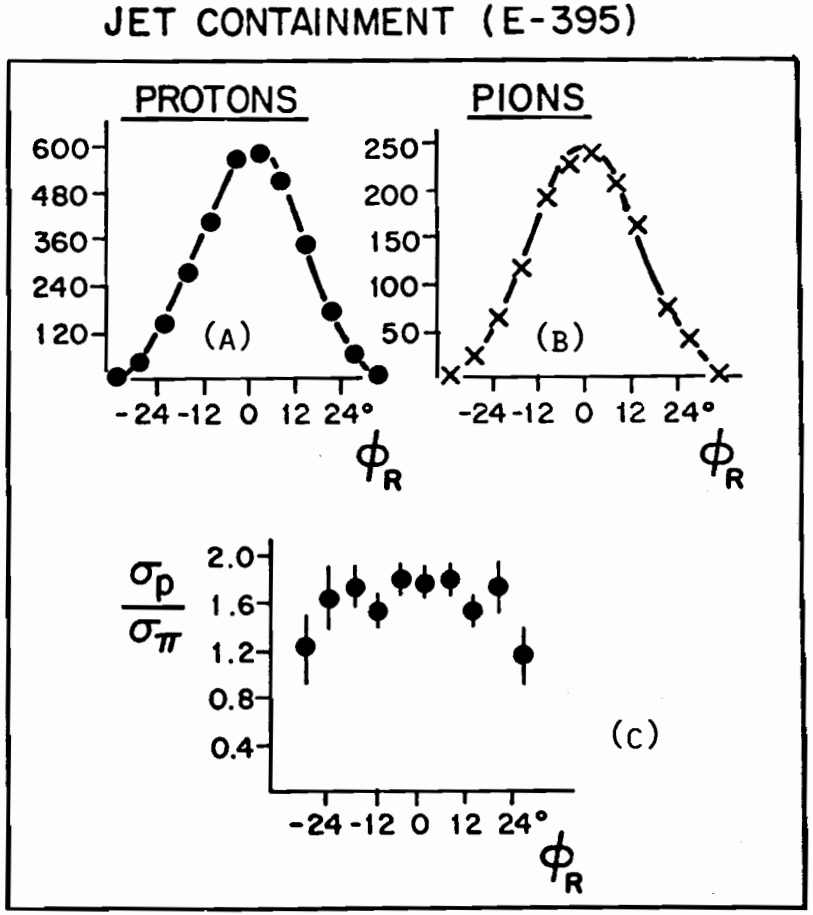

FIG. 21 (a) and (b) give dN/dφ (see text). The edge of the calorimeter is at $\phi \approx \pm 43^\circ$. (c) The ratio R_{jet} (Eq. 8.1) as a function of φ.

vector from the edge of the calorimeter, within a band of fixed θ^*_{jet}. Plots a and b in Figure 21 show the $dN/d\phi$ distributions for proton jets and pion jets, in the band illustrated in the right arm in Figure 17; ϕ_R is zero at the center of the band. (Note that Figure 17b is for 2-arm-sum triggered events, while Figure 21 is for events triggered with a single-arm (R) trigger.)

In Figure 21, plots a and b show that for fixed p_T(jet) and $\theta^*_{(jet)}$ the density of events $dN/d\phi_R$ falls rather rapidly as the jet axis goes away from the center of the calorimeter arm. This fall is presumably due to the decreased detection efficiency for events whose jet axes lie near the calorimeter edge. What is of considerable importance is that $dN/d\phi_R$ falls in almost exactly the same way for proton jets and for pion jets.

This result has several important implications and consequences [11]:

(1) First it implies that the pion jets and proton jets in this p_T and θ^* range have very similar fragmenting distributions--i.e., very similar multiplicities and similar "sizes".

(2) This result also suggests that the pion jets and protons jets, in this p_T and θ^* range, may come from virtually identical constituents. That is, if both quark jets and gluon jets are being detected, then either the quark jets and gluon jets are very similar in "size", or else the ratio of quark jets to gluon jets must be quite similar for the observed proton and pion jets.

(3) The ratio R_{jet} , $= \sigma_p/\sigma_\pi$ (Eq. 8.1), is quite constant over a wide range of ϕ_R , as seen in figure 21c. Since R is a sensitive function of p_T , as seen in Figure 20, the fact that it is constant while both $dN/d\phi_R$ drop several-fold suggests that the "true" p_T of the jet is not appreciably different from the measured p_T , over a wide range of ϕ_R , even though the calorimeter acceptance has dropped by a large factor at larger $|\phi_R|$.

In this last point, one has additional evidence that a calorimeter trigger has the surprising property of giving a fairly accurate measurement of the true momentum of a jet, as long as one has a detector solid angle $\Delta\Omega$ of $\sim$ 1 sr or more. That is, even for $\Delta\Omega$ as small as 1 sr (jet axis no less than $\sim$ 25 - 30^o from the edge of the calorimeter), and even for jet p_T as small as $\sim$ 2.5 GeV/c (the value in Figure 21), the evidence indicates that the jet containment is sufficiently good (because of the Dris effect) to give reasonably accurate results for the jet momentum.

9. PION STRUCTURE FUNCTION INFORMATION

With this evidence that jets can be reasonably cleanly defined and contained, the E-395 group have studied the angular and momentum distribution

of 2-jet events from πp and pp collisions in detail and have reported resulting information on the structure function for quarks and anti-quarks in the pion[11]. The basic approach used is to compare proton and pion cross sections for di-jet production, and to attempt to relate the ratio of cross sections to the ratio of parton intensities--i.e., to the ratio of structure functions. This method makes use of the kinematic relations indicated in Figure 22, together with the information on the similarity of proton jets and pion jets discussed in Section 8.

If only one species of parton-parton collision occurred, say for example $qq \to qq$ through gluon exchange, then the ratio of quarks in the proton to quarks in the pion, at a given x_1 (beam parton x), would be given by measuring the 2-jet cross section ratio

$$\frac{\sigma_p}{\sigma_\pi} = \frac{\sigma(pp \to \text{jet L} + \text{jet R} + X)}{\sigma(\pi p \to \text{jet L} + \text{jet R} + X)} , \qquad (9.1)$$

at fixed $\vec{P}_{TL}$ and $\vec{P}_{TR}$. Each choice of p_T magnitude, and of angles θ_L and θ_R, selects a particular x_1. In this single-species case, σ_p/σ_π would be equal to the structure function ratio for that x_1, $f_{q,p}(x_1)/f_{q,\pi}(x_1)$.

In the actual case, however, many additional factors enter, when one tries to understand how to relate the σ_p/σ_π of (9.1) to the ratio of structure functions. These questions are discussed in detail in reference (11). Here we concentrate on one essential point.

The proton and pion contain partons of many different species--valence quarks, sea quarks, and gluons. In principle the cross section ratio (9.1) involves the ratio of sums over the various parton species which can give rise to jet pairs, with each type of collision contributing with appropriate factors for structure functions, parton-parton scattering cross sections, and detection efficiencies.

One prominent question which arises concerns the contribution of gluon collisions (qG, $\bar{q}$G, and GG) to the jet pair events. If gluons have different structure functions from quarks, if cross sections for gluon collisions have different dependences on the s' and t' parton-parton Mandelstam variables than do cross sections for quark-quark collisions, if gluon jets have notably different characteristics and detection efficiencies than quark jets, then the σ_p/σ_π ratio will give only some average over the ratio of structure functions in proton and pion.

In reference (11) the authors report that the ratio of cross sections, σ_p/σ_π, is found to depend, approximately, only on the x of the beam parton, in the x-range studied, 0.25 to 0.55 (Figure 23). This result, together with the similarities found for the character of proton jets and pion jets (Section 8

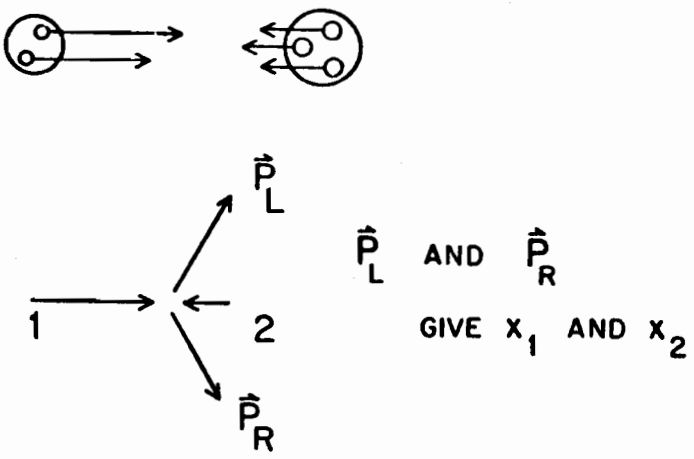

FIG. 22 KINEMATICS USED FOR STRUCTURE FUNCTION STUDY

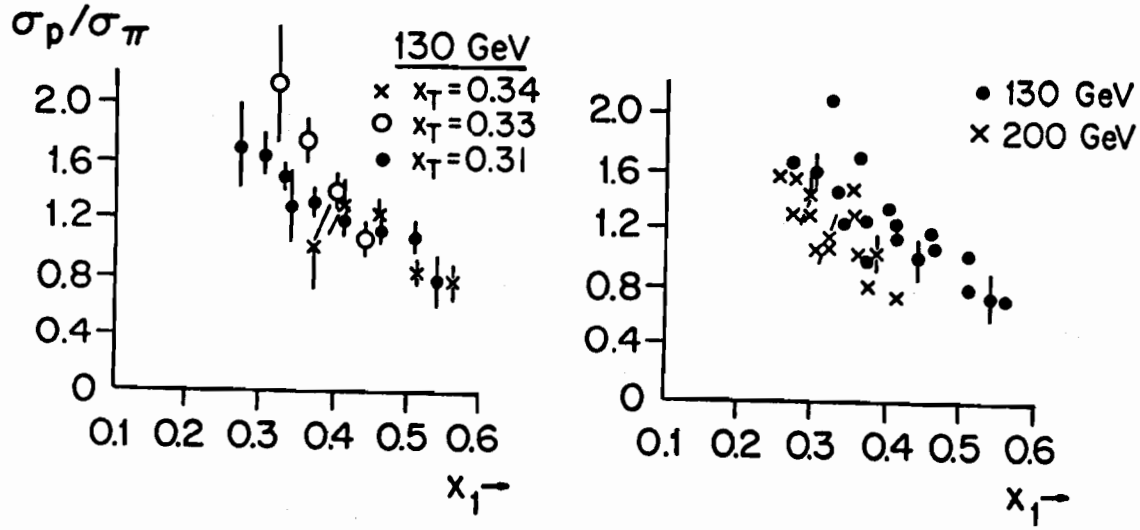

FIG. 23 Ratio $R_{2\text{-jet}}$ (Eq. 9.1). x_T = (PTL + PTR)/$\sqrt{s}$.

and reference (11)), leads the authors to conclude that

$$\frac{\sigma_p}{\sigma_\pi} \simeq \frac{f_{q+\bar{q},p}(x)}{f_{q+\bar{q},\pi}(x)} . \qquad (9.2)$$

They also point out that the fact that σ_p/σ_π is approximately independent of all variables except x_1 might indicate that in the x-range studied the ratio of gluons to quarks (plus antiquarks) in the proton is approximately the same as in the pion. If this is so, then σ_p/σ_π also gives the ratio of gluon structure functions, $f_{g,p}(x)/f_{g,\pi}(x)$ [55].

The results for $f_{q+\bar{q},\pi}(x)$ are shown in Figure 24, where they are also compared with previous theoretical predictions by Farrar [56] and by Field and Feynman [57]. The reasonably close quantitative agreement with the theoretical estimates might indicate that the 2-jet data do give information on parton scattering and on the quark distribution in the pion. Further evidence bearing on this interpretation is discussed below in Section 11.

10. PARTON TRANSVERSE MOMENTUM INFORMATION

In Section 6 we discussed the fact that the unbalance of p_T values in the 2-jet events appears to give information on parton transverse momentum [1,8,9]. The analysis of this unbalance is simplest for events taken with the double-arm L+R trigger. We give here some details of the current state of this analysis [58].

In a 2-jet event the two jets have transverse momenta $\vec{P}_{TL}$ and $\vec{P}_{TR}$ which do not in general exactly cancel. The sum of these momenta is the di-jet transverse momentum, $\vec{P}_T$. (We use P_T to indicate the di-jet, p_T to indicate individual jets or particles.) As shown in Figure 25 and as explained in reference (12), the x-component of P_T has an rms value which is closely related to the rms (2-dimensional) k_T of each of the two partons whose collision produces the di-jet.

Figure 26 shows the experimental $(P_{TX})_{rms}$ values for di-jets over a range of values of p_T (average of P_{TL} and P_{TR}) and of beam energy, for pp collisions. Now the unbalance, $(P_{TX})_{rms}$, receives a contribution from calorimeter resolution, and from missing jet fragments, as well as from parton transverse momentum k_T. These instrumental effects have been calculated using a Monte-Carlo model (see Section 5) which closely simulates many experimental features of the data. The Monte-Carlo results are also shown in Figure 26. When these results are subtracted, in quadrature, from the raw data points in Figure 26, resolution-corrected values result, shown in Figure 27.

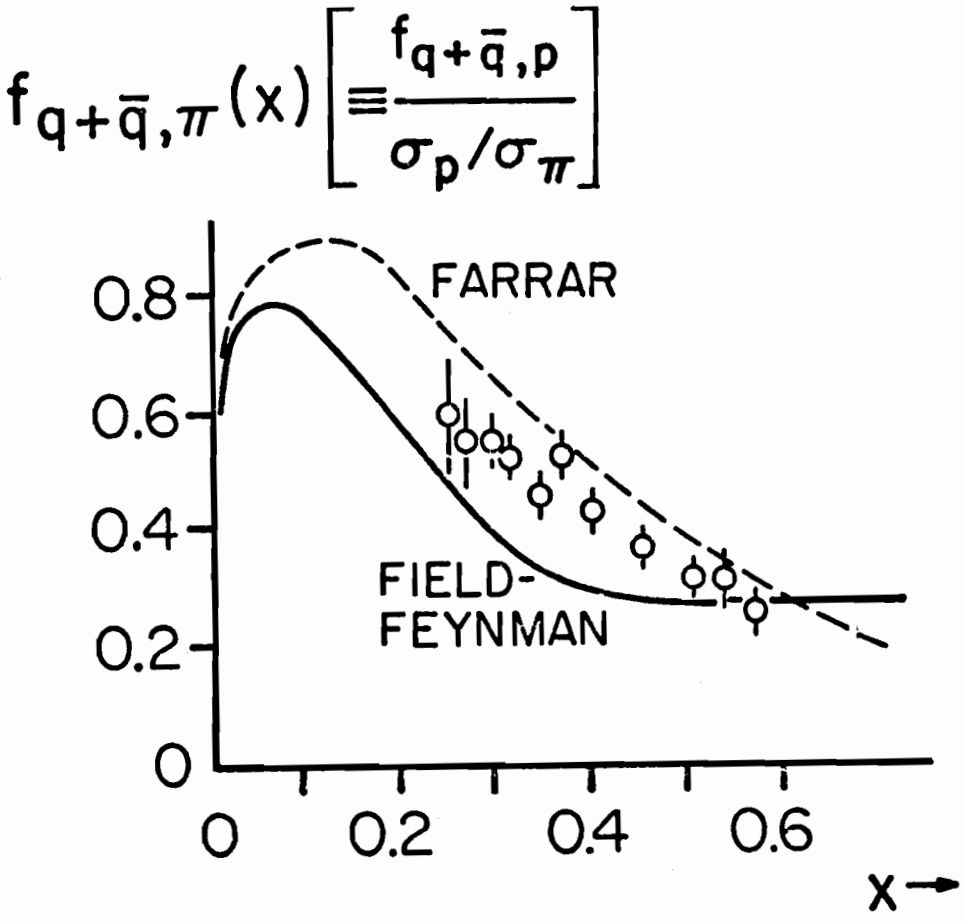

FIG. 24 RESULTS OF THE E-395 ANALYSIS FOR THE QUARK-PLUS-ANTIQUARK STRUCTURE FUNCTION OF THE PION

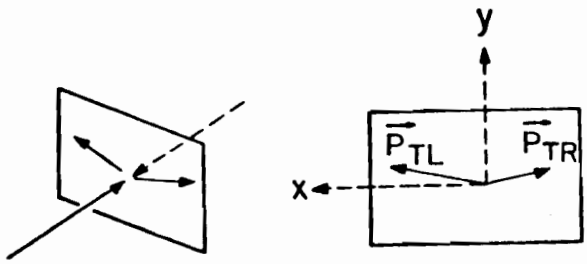

$$(\vec{P}_T)_{\text{di-jet}} = \vec{P}_{TL} + \vec{P}_{TR}$$

$$\langle P_{TX}^2 \rangle^{1/2} = (k_T)_{\text{rms(each parton)}}$$

FIG. 25

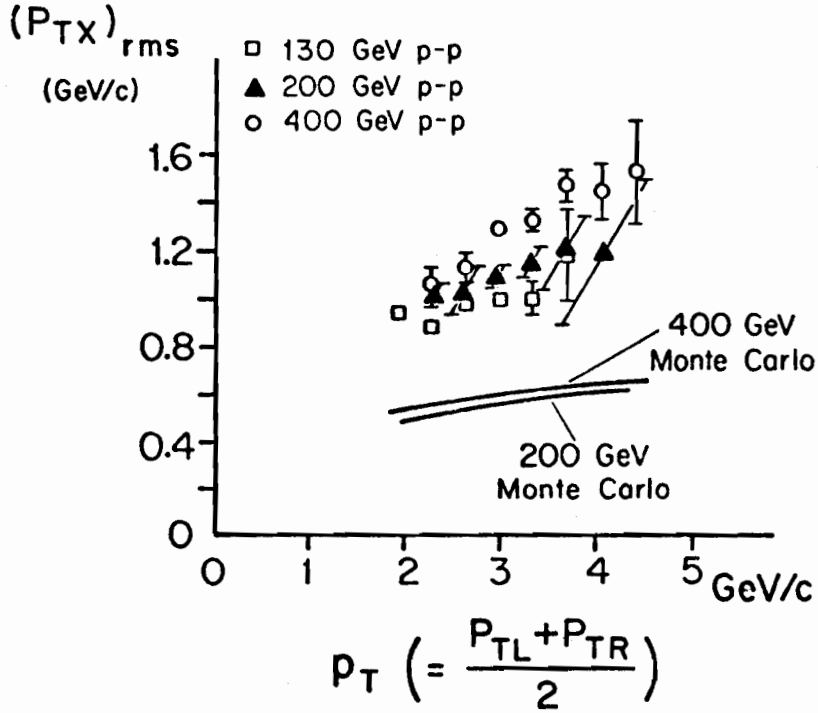

FIG. 26 $(P_{TX})_{rms}$ gives the rms unbalance of the x-component of $(\vec{P}_T)_{\text{di-jet}}$.

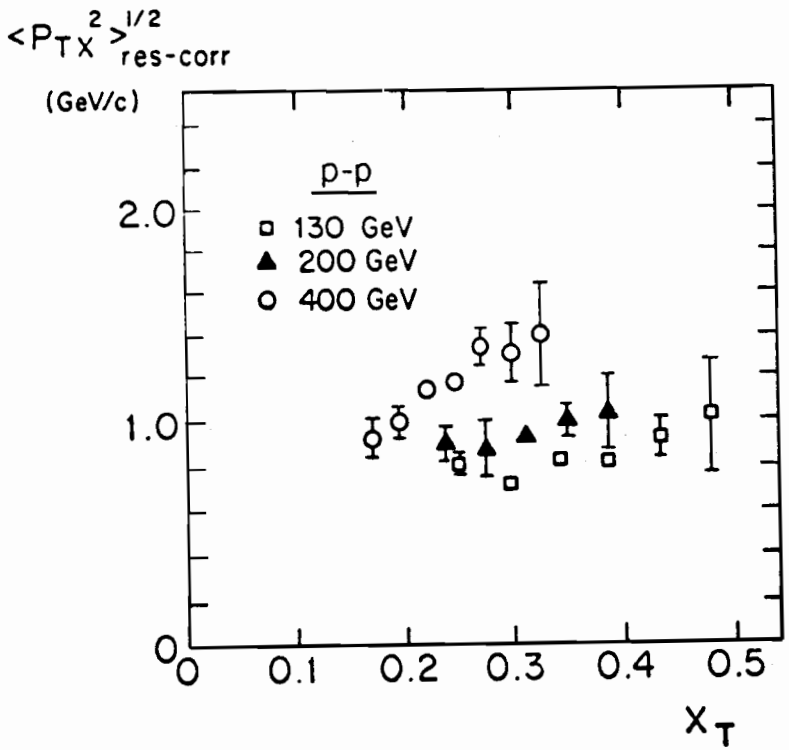

FIG. 27 $(P_{TX})_{rms}$ after correction for instrumental resolution effects.

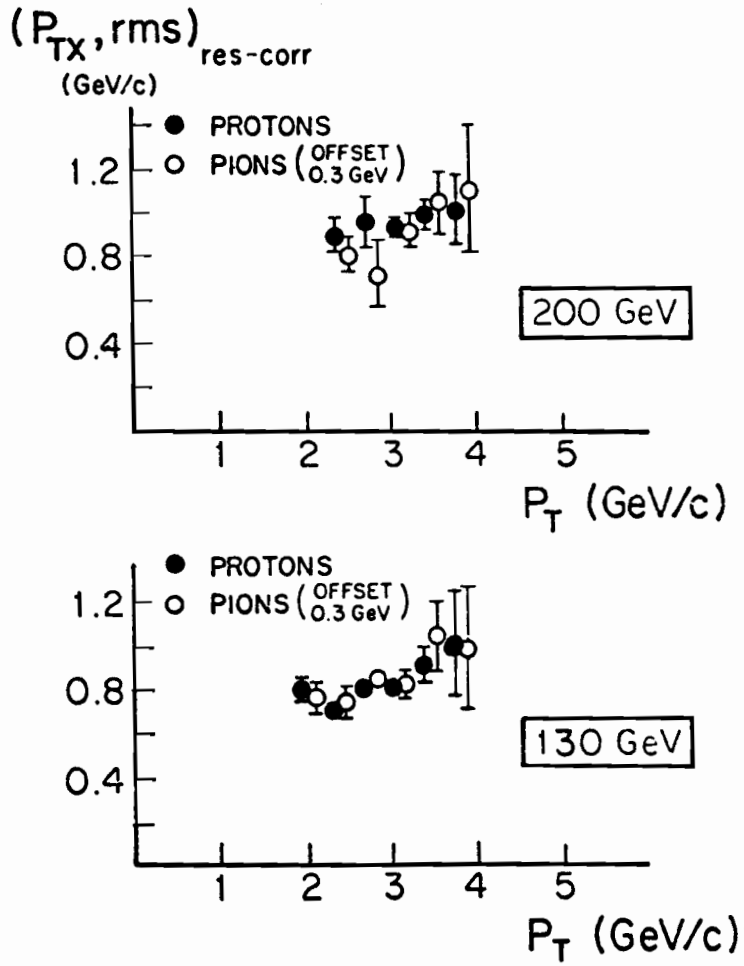

FIG. 28 Comparison of pp and πp results, for the resolution-corrected $(P_{TX})_{rms}$. The pion data points are plotted at shifted p_T values, for clarity.

The results shown in Figure 27 show an increase in $(P_{TX})_{rms}$ with s, and some indication of an increase with p_T. The magnitude of these resolution-corrected results, and the increase with s, for these di-jets, are very similar to what has been observed for transverse momentum of di-muons in hadron collisions. This comparison is discussed further, in Section 11.

Although the general nature of the P_T information obtained from the di-jet results is similar to that obtained from di-muons, the basic processes have certain important differences. One of those differences appears to be responsible for an important difference observed in di-jet and di-muon results for $(P_T)_{rms}$. Namely, for di-muons the $(P_T)_{rms}$ values for proton-induced events and pion-induced events are different[59,60]; but for di-jets the $(P_T)_{rms}$ values for proton-induced and pion-induced events are not different. The di-jet results are shown in Figure 28. The difference, in this respect, between di-jet and di-muon results, is readily understandable. In the di-jet process similar constituents are colliding, in πp and pp cases (Section 9). In di-muon production, on the other hand, theory suggests that different species of collisions dominate for pion-induced and proton-induced di-muons, in the kinematic region studied[59].

11. SIMILARITY OF DI-JET AND DI-MUON RESULTS, AND IMPLICATIONS

The analysis of the 2-jet events discussed in Sections 9 and 10 gives results for the quark(plus antiquark) structure function of the pion, and for the (resolution-corrected) transverse momentum of the di-jet, $(P_{TX})_{rms}$. It is interesting to see how these results compare with information obtained from di-muon production.

A. Comparison of pion structure function information.

Pion structure function information has been published from the di-jet experiment[11] and from a di-muon experiment[61]. Both experiments report some systematic uncertainty of the order of 20% in the quantitative results. The results, plotted with an adjustment of 25% in absolute scale, are found to agree very closely with each other, as seen in Figure 29. (Fig. 29 shows the results plotted out to $x = 0.6$. The di-muon experiment also gives results at larger x, out to $x \simeq 1.0$.)

The agreement for the two experiments not only as to the shape of f(x) but also as to its absolute magnitude (within experimental uncertainties) offers substantial support for the conclusion that in both experiments the data give information on the quark structure function of the pion. For the di-muon experiment this conclusion indicates that the di-muons are produced by a

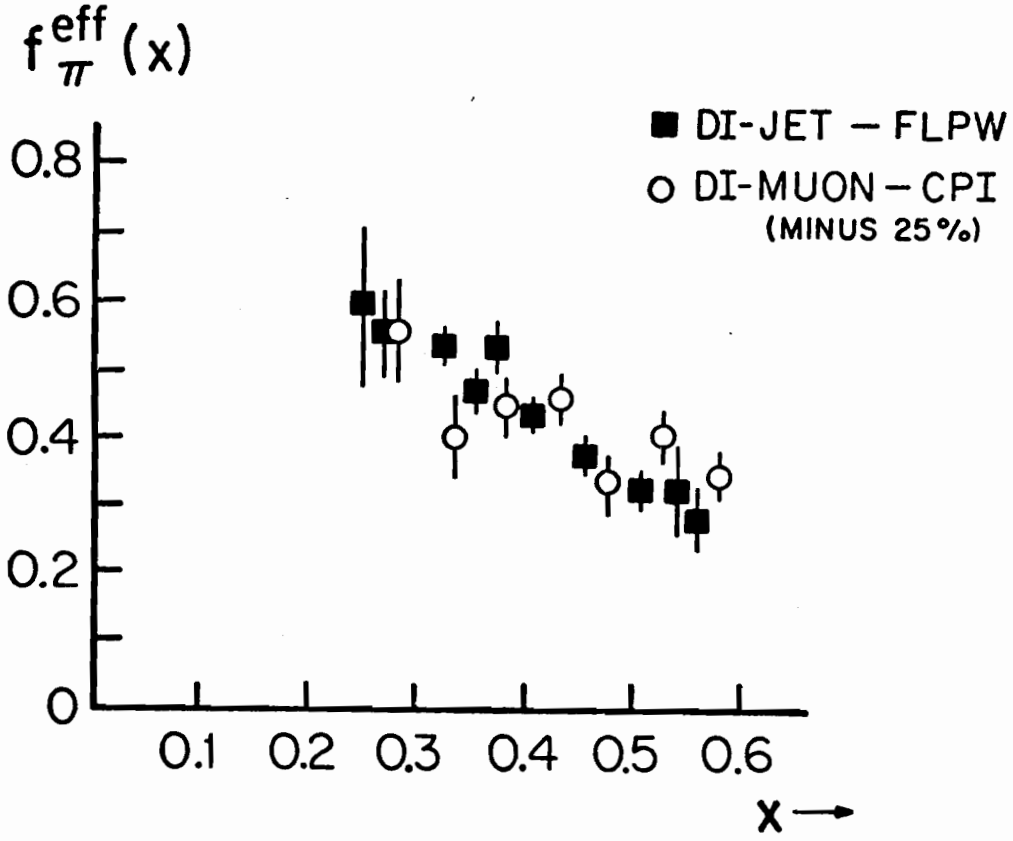

FIG. 29 Comparison of the effective quark-plus-antiquark structure function of the pion, as determined from di-jet (Ref. 11) and di-muon (Ref.61) experiments. The di-muon results of Ref. 61 have been decreased 25%, for this plot.

Drell-Yan type process, in which the incident parton is a quark (or valence anti-quark), and that even with the residual uncertainties in the analysis[61] one can obtain closely the quark structure function of the pion from di-muon data. For the di-jet experiment this conclusion indicates that the interpretations made in the di-jet analysis are probably not greatly in error, --and that the di-jet events do in fact correspond closely to parton-parton scattering, with the measured momentum of each jet corresponding closely to the momentum of the scattered parton.

B. Comparison of k_T (parton transverse momentum) information.

($P_{T,rms}$) di-muon results have been obtained for a wide range of di-muon masses and beam energies, in pN collisions (N = nucleus) and πN collisions. If one interprets these P_T values as due to the combination (in quadrature) of individual parton k_T values, then if the two initial partons contribute equally one has

$$(k_T)_{rms} = (P_{T,rms})/\sqrt{2}. \qquad \text{(DI-MUONS)} \qquad (11.1)$$

For di-jet events, one measures most readily not $P_{T,rms}$ but $P_{TX,rms}$; in this case one has, correspondingly[12],

$$(k_T)_{rms} = (P_{TX,rms}). \qquad \text{(DI-JETS)} \qquad (11.2)$$

For both types of experiment, $P_{T,rms}$ is found to vary with di-muon mass ($M_{\mu\mu}$) or di-jet mass ($\simeq 2\ p_T$), and with s. Before comparing the k_T values from the two types of experiments, however, several points must be noted.

(1) The di-muon data obtained at Fermilab have all been obtained with non-hydrogen targets, while the di-jet data have been obtained with a hydrogen target.

(2) $P_{T,rms}$ values for di-muon data at given s have been found to level off as $M_{\mu\mu}$ increases, above $M_{\mu\mu} \simeq 3$ to 5 GeV, while no such clear leveling off occurs for di-jet data.

(3) Proton-induced and pion-induced di-muons show different $P_{T,rms}$ values (for higher $M_{\mu\mu}$ values), whereas no difference is seen for di-jet results.

(4) For the di-jet process there are several types of corrections which must be applied to $P_{T,rms}$ before k_T values can be extracted. The instrumental resolution effect discussed in Section 10 appears to be the dominant correction. There are however several additional corrections, which appear to be small but not negligible[58].

Besides the differences just noted, there are two major differences in the nature of the di-muon and di-jet production processes. First, in di-muon production there is no strong "final-state-interaction" effect--the virtual

photon, or the di-muon which results, escapes from the hadronic production region without interacting strongly with the remaining partons. In di-jet production, on the other hand, presumably two partons are scattered, carrying total non-zero $(P_T)_{\text{di-parton}}$ before the scatter, but then produce two jets which together can have a larger $(P_T)_{\text{di-jet}}$, because of further strong interactions (and/or radiative gluon effects) occurring after the scattering but before the final jets emerge.

Secondly, in the two different processes not only do quite different detailed diagrams enter, but different parton species may play major roles. In the di-muon process, e.g., it is thought that antiquark-quark annihilation may be the dominant process for πN collisions but not for pN[59]; and in the di-jet process we do not at present know what contribution is present from qG (quark-gluon) and GG collisions as compared to qq collisions.

In view of all of these differences, one should perhaps hardly expect the $(k_T)_{\text{rms}}$ obtained from di-muons (11.1) to be closely the same as that obtained from di-jets (11.2). Clearly the comparative values should be examined over a wide range of mass and of s and for different incident and target hadrons, before clear conclusions are drawn. I give here a comparison at a single sample point--a more detailed comparison will be given elsewhere.

For 200 GeV di-muon production using incident protons on Pt, Yoh et al.[62] give $\langle P_T \rangle \simeq 0.97$ GeV/c for $M_{\mu\mu} \simeq$ 6-8 GeV, or $P_{T,\text{rms}} \simeq 1.09$ GeV/c. This corresponds (11.1) to

$$(k_T)_{\text{rms}} \simeq 0.77 \text{ GeV/c.} \qquad \text{(DI-MUONS)} \qquad (11.3)$$

(p-Pt, 200 GeV, $M_{\mu\mu} \simeq 6 - 8$ GeV)

For di-jet production, at 200 GeV and $p_T = 3$ GeV/c ($M_{\text{di-jet}} \simeq 7$ GeV), E-395 obtain $(P_{TX,\text{rms}})_{\text{resolution-corrected}} \sim 0.94$ GeV/c. A major additional correction which must be made to this value is a reduction for a "t'-spreading" effect[63]. This effect is estimated to increase $P_{TX,\text{rms}}$ by 10 to 15%[58,64]. Correction for this effect reduces $(P_{TX,\text{rms}})$ to $\sim$ 0.82 to 0.85, and gives

$$(k_T)_{\text{rms}} \simeq 0.82 \text{ to } 0.85 \text{ GeV/c.} \qquad \text{(DI-JETS)} \qquad (11.4)$$

(p-p, 200 GeV, $M_{\text{di-jet}} \simeq 7$ GeV)

In view of all of the uncertainties and differences noted above, it is perhaps surprising that the di-muon and di-jet experiments give k_T values so close as those in (11.3) and (11.4).

C. Implications of the similarity between di-jet and di-muon results.

We have discussed above the close similarity in results for the pion quark structure function and for parton k_T, from these two quite different kinds of

experiments. In spite of some difficulties and ambiguities in the interpretation of the di-muon data, a very strong case has developed for the interpretation of these data in terms of $q\bar{q}$ annihilation, the original Drell-Yan process, as modified by current theoretical ideas on QCD effects[21,59]. If we take this Drell-Yan interpretation as being better established than the interpretation of jet events, then the close similarity of results would imply that the measurement and analysis of di-jet events, with large solid angle calorimeters, gives quite direct information on parton-parton scattering. This appears to indicate that jet events do in fact correspond to parton-parton scattering, that the typical jet has a measured momentum quite close to that of the scattered parton, and that the conclusion in Section 9 and reference (11) concerning the interpretation of di-jet π/p cross section ratios in terms of quark structure function ratios is approximately correct. If all of these conclusions are correct, then the study of hadron jets in hadron collisions, and particularly of jet pairs, provides a practical and unique means for the study of the strong interaction in parton-parton scattering.

12. SEARCH FOR GLUON JETS

Given the existing evidence that 2-jet events correspond to parton-parton scattering, it is quite important to investigate whether one can distinguish gluon jets from quark jets. QCD theory suggests that gluon jets should be "softer" than quark jets--that the gluon jets should have higher multiplicity, and a relatively larger number of fragments at wider angles from the jet axis[65,66]. Moreover, gluon structure functions are expected to be more concentrated at small x than are quark structure functions[66,67]. Motivated by these suggested differences in gluon/quark jet properties and structure functions, the E-395 group have searched in several ways for corresponding effects which might be expected to be observed in di-jet distributions. Thus far these searches, all based on the possible difference in multiplicity for quark jets and gluon jets, have all given negative results.

One search method is described here as an example. Figure 22 represents the kinematics for parton-parton scattering. If it is true that gluon structure functions are relatively more concentrated at small x, then one may hope that when x_1 and x_2 are both large it is quark-quark scattering which dominates but that as one goes to the domain of large-x_1/small-x_2 the contribution from quark-gluon collisions will grow relatively larger. If this contribution does grow larger, and if gluon jets have greater multiplicity than quark jets, then for fixed p_T one may expect to find that the jet multiplicity increases as one goes to the smaller-x_2 region.[68]

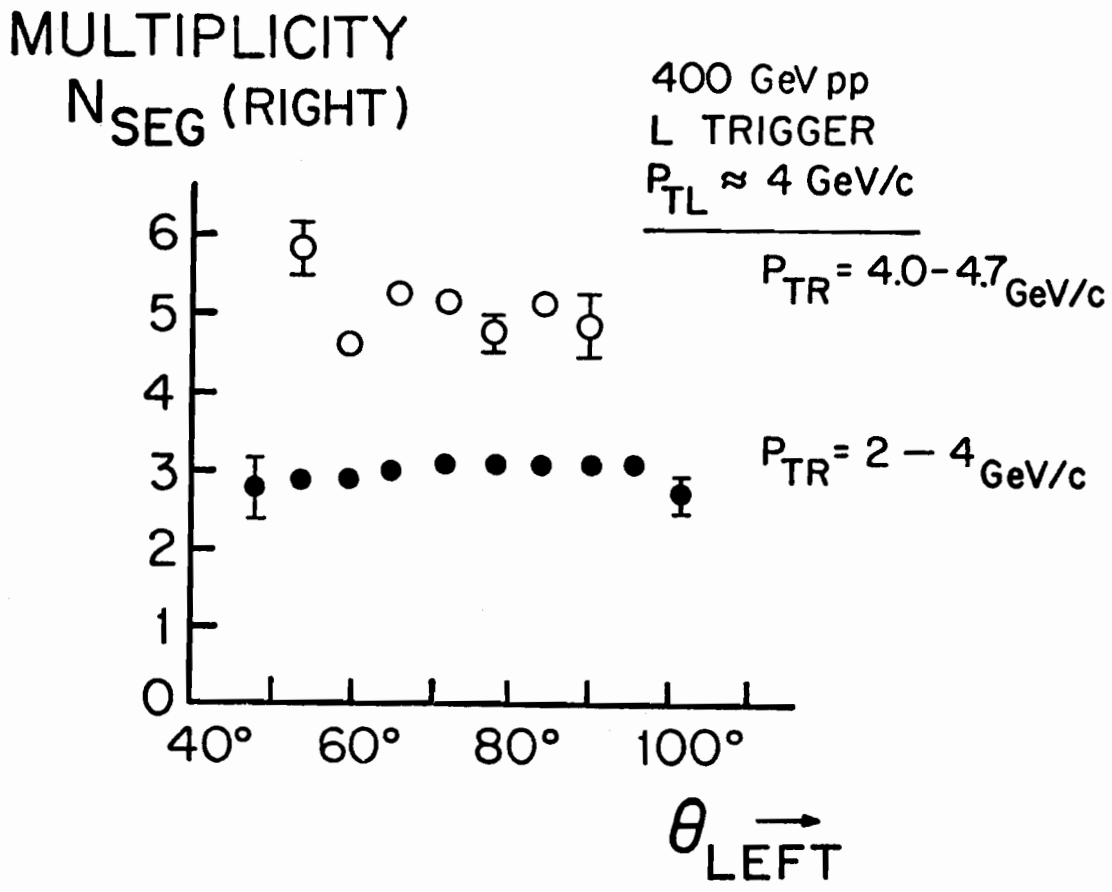

FIG. 30 Multiplicity of right-arm (away-side) jet, as a function of θ(left jet); θ(right jet) is kept fixed at $\sim 90^{\circ}$.

Figure 30 shows the results of such a search. In order to avoid effects of detector acceptance on jet multiplicity, the multiplicity is measured for jets of fixed p_T(right), restricted to point at the central fiducial region in the right arm, and the right arm is used as an away-side arm, not included in the trigger. Thus the trigger is taken as an L (left arm) trigger, of fixed p_T but of varying angle θ(LEFT). From the discussion above, one might have expected to see the right-arm multiplicity increase as θ(LEFT) decreases. No such effect is seen.

It is difficult to place quantitative limits, from the results, on the possible magnitude of any difference in the multiplicities for gluon jets and quark jets. The experimental results involve a folding of many effects--structure functions, parton scattering cross sections, and jet detection efficiencies. Nevertheless, in the light of the negative result of this search and of other related searches for multiplicity differences[69], two comments are in order. First, the multiplicity difference predicted by QCD[65,66] for gluon and quark jets is a prediction applicable in the limit of "very high" jet energies. It is not clear[70] at what minimum jet energies these calculations might become relevant. Second, only one calculation is known to me which directly addresses the question of the possible multiplicities for quark and gluon jets at jet energies presently available experimentally. That calculation, by Sukhatme[71], gives the result that the multiplicities would be virtually indistinguishable at the jet energies involved in E-395.

It thus appears that searches for gluon-quark jet differences based purely on multiplicity may not be very fruitful, and that it may be necessary instead to use flavor information in order to try to distinguish gluon and quark jets. A possible indication of such flavor differences may be present in charge correlations observed by the CCHK group[72], for events which would correspond to the same kind of large-x_1/small-x_2 collisions discussed above. As noted in their report, however, the charge correlations observed, which indicate decreasing average jet charge for decreasing x_2, could correspond to effects of sea quarks as well as of gluons.

13. CONCLUSIONS

Since the first observation of unexpectedly large cross sections for production of high p_T particles at the ISR, a long and difficult series of experiments, also at the ISR, slowly built up an accumulation of evidence that the high p_T particles were produced in jet-like groups. Thus by the time calorimeter triggered experiments came into operation, at Fermilab, one could

confidently expect to find large cross sections for multi-particle high p_T groups. These large cross sections were first found by direct measurement in experiment E-260.

The properties of these high-p_T groups have recently been greatly clarified by additional information from ISR experiments, and by the calorimeter experiments E-260 and E-395 at Fermilab. Two major questions were initially (1) how does one define a jet, and (2) can jets be defined and measured cleanly enough so that the jet momentum vector can be expected to correspond closely to the momentum of a scattered parton? The calorimeter experiments have shown that because of the rapidly falling p_T spectrum a trigger bias (Dris effect) operates in such a way that those jets which are detected with a calorimeter trigger are measured relatively accurately--there is relatively little jet momentum and energy outside of the trigger solid angle.

In experiment E-395 2-jet events have been detected clearly for the first time, and a number of new results have been found.

(1) A peak in the away-side p_T spectrum has been seen for the first time, in single-arm triggers.

(2) Approximate p_T balance for 2-jet events is found to occur.

(3) A highly important angular correlation difference between πp-produced jet pairs and pp-produced jet pairs has been seen. This difference, together with p_T balance and coplanarity, suports the interpretation that the 2-jet events come from parton-parton scattering.

(4) The 2-jet events were analyzed to give the first direct information on the quark structure function of the pion.

(5) The unbalance in p_T for the 2-jet events was analyzed to give information on parton transverse momentum k_T as observed in parton-parton collisions.

The structure function results, and the parton transverse momentum results, have been compared with results obtained from di-muon production. The results agree surprisingly well. (There is a significant difference as regards parton k_T for pion-induced as compared to proton-induced reactions, but this difference is readily understandable and reasonable.) This agreement implies that the measurement of di-jet events with large solid angle calorimeters gives quite direct information on parton-parton scattering, with the typical jet having a measured momentum quite close to that of the scattered parton. It thus appears that the study of hadron jet events in hadron collisions, and particularly of jet pairs, provides a practical and unique means for the study of the strong interaction between partons.

Finally, in the further pursuit of this field it is quite important to try to distinguish gluon jets from quark jets. Initial efforts to distinguish them on the basis of a difference in multiplicity have given negative results.

The implication is that for presently studied jet energies there is not a major difference in multiplicities, for quark jets and gluon jets. Further efforts to distinguish these two types of jets, at these energies, should make use of parton flavor information.

14. ACKNOWLEDGMENTS

I wish to thank E. Malamud and G. C. Fox for generously supplying information on E-260 analysis and results; they are not responsible however for my detailed comments.

The work on E-395, and the results reported from it, represent major initiatives and contributions by all of the members of the FLPW collaboration.

Finally, I have benefited also from discussion with many other physicists. I particularly want to express my appreciation to J. D. Bjorken for a number of such discussions, which provided a major stimulus for this work.

The work on E-395, and the preparation of this report, were supported in part by the U. S. Department of Energy.

REFERENCES AND FOOTNOTES

1. G. C. Fox, in Particles and Fields - 1977, AIP Conference Proceedings No. 43, edited by P. A. Schreiner et al. (AIP, New York, 1978), p. 193.
2. J. D. Bjorken, Phys. Rev. D8, 4098 (1973).
3. S. Berman, J. Bjorken, and J. Kogut, Phys. Rev. D4, 3388 (1971).
4. C. Bromberg et al., Phys. Rev. Lett. 38, 1447 (1977).
5. C. Bromberg et al., Nucl. Phys. B134, 189 (1978).
6. C. Bromberg et al., Phys. Rev. Lett. 42, 1202 (1979).
7. Fermilab--P. Gollon; Lehigh--A. Kanofsky, G. Lazo; Pennsylvania--L. Cormell, M. Dris, W. Kononenko, B. Robinson, W. Selove, B. Yost; Wisconsin--M. Corcoran, A. Erwin, E. Harvey, R. J. Loveless, M. Thompson.
8. L. Cormell et al., Evidence for Jets, and for Correlated Jets, in High P_T Events, Univ. of Pennsylvania Report UPR-24E, October 1977 (unpublished).
9. A. R. Erwin, in New Results in High Energy Physics, 1978, AIP Conference Proceedings No. 45, eds. R. S. Panvini and S. E. Csorna (AIP, New York, 1978), p. 64.
10. M. D. Corcoran et al., Phys. Rev. Lett. 41, 9 (1978).

11. M. Dris et al., Phys. Rev. D19, 1361 (1979).

12. M. D. Corcoran et al., Physica Scripta 19, 95 (1979).

13. W. Selove, in Proc. 19th Intl. Conf. High Energy Physics, edited by S. Homma et al. (Physical Society of Japan, Tokyo, 1979), p. 165.

14. B. T. Yost et al., IEEE Transactions on Nuclear Science, Vol. NS-26, No. 1, p. 105 (1979).

15. W. Selove et al., in Proceedings of the Calorimeter Workshop, 1975, editor M. Atac (Fermilab, Batavia, 1975), p. 271.

16. W. Selove, W. Kononenko, and B. Wilsker, Nucl. Instr. and Methods 161, 233 (1979).

17. This figure comes from detailed analysis of the data, and from detailed comparison of the experimental results with the results from Monte Carlo calculations.

18. J. Rohlf, talk presented at the Caltech Workshops on High Energy Physics, February 1979. I thank G. C. Fox for providing me with information on the material presented in this talk.

19. D. Antreasyan et al., Phys. Rev. Lett. 38, 112 (1977).

20. R. P. Feynman, R. D. Field, and G. C. Fox, Phys. Rev. D18, 3320 (1978).

21. R. D. Field, Physica Scripta 19, 131 (1979).

22. J. D. Bjorken, SLAC-PUB-1777, July 1976.

23. For discussion of these predictions, and for recent reviews of high p_T and jet physics, see references (2), and (24)-(27).

24. D. Sivers, S. Brodsky, and R. Blankenbecler, Phys. Reports 23C, 1 (1976).

25. S. D. Ellis, M. Jacob, and P. V. Landshoff, Nucl. Phys. B108, 93 (1976).

26. S. D. Ellis and R. Stroynowski, Rev. Mod. Phys. 49, 753 (1977).

27. M. Jacob and P. V. Landshoff, Phys. Reports 48C, 285 (1978).

28. M. Jacob, Physica Scripta 19, 69 (1979).

29. G. Hanson, talk presented at 13th Rencontre de Moriond, 1978 (and SLAC-PUB-2118).

30. See reports from the Symposium on Jets in High Energy Collisions (Nordita/NBI, July 1978), published in Physica Scripta 19, No. 2, February 1979, and particularly references (31)-(34).

31. A. G. Clark et al., Physica Scripta 19, 79 (1979).

32. A. L. S. Angelis et al., ibid., 116.

33. J. C. Vander Velde et al., ibid., 173.

34. W. G. Scott, ibid., 179.

35. The data sample used did require the total right-arm p_T to be above a hardware threshold of about 3 GeV/c.

36. Monte Carlo studies using a jet model similar to that corresponding to Figure 8, and using measured properties of the calorimeter array, show that this definition gives a good approximation to the actual number of particles in the cluster.

37. M. A. Dris, Nucl. Instr. and Methods 158, 89 (1979).

38. Corrections for calorimeter energy resolution have been made only roughly for these away-side p_T spectra. A more accurate correction will cause the away-side peak to increase somewhat in p_T.

39. CCOR reports at Copenhagen, ref. (32), and at Tokyo (by R. L. Cool).

40. G. C. Fox, private communication.

41. B. L. Combridge, Phys. Rev. D12, 2893 (1975).

42. M. Della Negra et al., Nucl. Phys. B127, 1 (1977).

43. G. Finnochiaro et al., Phys. Lett. 50B, 396 (1974).

44. K. Eggert et al., Nucl. Phys. B98, 73 (1975).

45. F. W. Büsser et al., Phys. Lett. 51B, 306 (1974).

46. M. Jacob and P. V. Landshoff, Nucl. Phys. B113, 395 (1976).

47. R. Blankenbecler, S. J. Brodsky and J. F. Gunion, Phys. Rev. D18, 900 (1978).

48. Because of the finite granularity of the E-395 detector it is not possible to obtain an unambiguous measurement of the multiplicity. The multiplicity for Figure 14 is calculated in the same way as for Figure 10. See also footnote (36).

49. For a display of similar data without the software cut, see references (8) and (12).

50. See references (43)-(45), and (32).

51. S. J. Brodsky, Physica Scripta 19, 154 (1979).

52. See discussion below on structure function results, parton transverse momentum results, and comparison between results from di-jet and di-muon production.

53. G. Donaldson et al., Phys. Rev. Lett. 36, 1110 (1976).

54. Note that the 1.4 factor does not mean that when one triggers on a single π^o there is an additional 40% p_T found in the calorimeter. The additional p_T found is in fact substantially less than 40%, in E-395. Interpretation of the ratio $x_T(\text{jet})/x_T(\pi^o)$ at fixed R(jet) requires consideration of many factors, and will be discussed elsewhere.

55. See reference 11, footnote 17.

56. G. R. Farrar, Nucl. Phys. B77, 429 (1974).

57. R. D. Field and R. P. Feynman, Phys. Rev. D15, 2590 (1977). The curve given by these authors was obtained using both theoretical arguments and a comparison of their quark-scattering and quark-fragmentation model with the experimental data of Donaldson et al., Ref. (53).

58. FLPW collaboration, to be published.

59. L. M. Lederman, in Proc. 19th Int'l. Conf. on High Energy Physics, Tokyo, 1978, p. 706.

60. K. J. Anderson et al., Phys. Rev. Lett. 42, 944 (1979).

61. C. B. Newman et al., Phys. Rev. Lett. 42, 951 (1979).

62. J. K. Yoh et al., Phys. Rev. Lett. 41, 684 (1978).

63. Events within a band of fixed PTL + PTR do not have constant parton scattering momentum transfer t'. As a result, the distribution of P_{TX}, similar e.g. to the distribution plotted in Figure 16, is broadened.

64. J. F. Owens, this conference.

65. K. Shizuya and S.-H. H. Tye, Phys. Rev. Lett. 41, 787 (1978).

66. There is a wide literature on this subject. See e.g. several of the reports from the Symposium on Jets, Copenhagen, 1978 (Physica Scripta, Vol. 19, No. 2, February 1979).

67. For a recent review and extensive references see R. D. Field, Ref. (21).

68. The suggestion for such an effect is due to D. Duke and H. Miettinen, private communication.

69. FLPW collaboration, to be published.

70. Informal discussion at this conference.

71. U. P. Sukhatme, Report LPTPE 78/36, Orsay, December 1978.

72. E. E. Kluge, Physica Scripta 19, 109 (1979).